

# Self-sealing of cracks in concrete using superabsorbent polymers

H. X. D. Lee, H. S. Wong\*, N. R. Buenfeld

Department of Civil and Environmental Engineering, Imperial College London, UK

## Abstract

Cracks in concrete can self-heal when exposed to prolonged wetting, but this is limited to narrow cracks. In practice, cracks  $> 0.2\text{mm}$  cause leakage and impair performance of structures. The potential of superabsorbent polymers (SAP) to self-seal such cracks was investigated via transport experiments, microscopy and modelling. Forty samples containing SAP and through-thickness cracks were subjected to  $0.12\text{wt.}\% \text{NaCl}$  at  $4\text{m/m}$  pressure gradient to simulate groundwater seepage. Results show that SAP can re-swell and seal cracks, for example in the case of  $0.3\text{mm}$  cracks reducing peak flow rate and total flow by 85% and 98% respectively. Increasing SAP dosage accelerates sealing, but imparts a strength penalty and this limits practical applications. Modelling suggests that the effectiveness of SAP can be enhanced by increasing its re-swelling ratio and particle size, and depressing its initial swelling. These variables increase the SAP exposed in a crack and the gel volume available to seal it.

*Keywords:* Durability (C); Permeability (C); Transport properties (C); Admixture (D); Superabsorbent polymer

\* Corresponding author: Tel.: +44(0)20 7594 5956, E-mail: hong.wong@imperial.ac.uk

## 1. Introduction

Concretes that are appropriately formulated and manufactured tend to be durable and have good resistance to water penetration. However, concrete is prone to cracking when exposed to structural loading or non-structural factors such as shrinkage, thermal effects and physiochemical reactions [1]. Indeed, a

24 fundamental principle of structural design is that concrete is cracked in the tension zone. Cracking causes  
25 leakage and affects watertightness, a critical serviceability requirement for many structures such as  
26 basements, retaining walls, reservoirs, dams, tunnels, pipelines and waste repositories. Cracks also act as  
27 pathways for aggressive agents, thereby accelerating deterioration mechanisms [2]. When cracks percolate,  
28 their influence on transport far outweighs that of capillary pores because of their larger size and shorter flow  
29 lengths. Therefore, cracks not only affect watertightness, but also long-term durability of concrete structures.

30 Cracks may heal when exposed to water [3-6, 44], but this is usually limited to narrow cracks ( $< 0.3$  mm)  
31 and dependent on many conditions such as mix composition, hydraulic pressure and temperature. The crack  
32 width limit for self-healing have been reported in some studies as 0.05 mm or below [6, 26]. According to  
33 current design guidance, concrete with cracks wider than 0.1 mm are expected to lose their watertight  
34 characteristics [2, 7, 8]. For example, ACI 224R-01 [7] recommends a crack width limit of 0.1 mm for water-  
35 retaining structures while Eurocode 2 [8] specifies that full thickness cracks should be less than 0.2 mm to  
36 limit leakage for structures exposed to an hydrostatic pressure gradient of  $\leq 5$ . Crack width can be limited by  
37 appropriate reinforcement detailing and provision of movement joints. However, special measures (e.g.  
38 external liners and pre-stressing) will be required if no leakage is permitted [8]. Methods such as surface  
39 coating, resin injection and integral water resisting admixtures are also often used to prevent leakage, but are  
40 not always effective, for example where there is significant movement, e.g. ground subsidence. Coatings  
41 deteriorate and require maintenance or reapplication. Water resisting admixtures are generally divided into  
42 hydrophobic or water-repellent chemicals, finely divided solids and crystalline materials. Finely divided  
43 solids and hydrophobic waterproofing admixtures are not considered effective in crack blocking. Some  
44 crystalline type admixture may seal very fine cracks, but only by reacting with unreacted cement and  
45 moisture to form crystalline products [9]. Many claims have been made concerning the effectiveness of these  
46 admixtures, but most reported tests focus on their effect on the reduction of permeability of un-cracked  
47 concrete. There seems to be a lack of independent data to substantiate their effect on crack blocking [10].

48 Advances in materials science have led to the development of a range of smart adaptive materials that  
49 heal themselves when cracks develop. A well-known example is a self-healing polymer containing

50 embedded microcapsules filled with a healing agent that is ruptured during cracking, releasing the agent into  
51 the crack where it mixes with a catalyst and polymerises [11]. There have been other similar attempts to  
52 induce self-healing in concrete using brittle glass fibres or capsules containing adhesives [12, 13]. More  
53 recently, much emphasis has been placed on developing bacteria-induced precipitation to heal cracks e.g. the  
54 work of Van Tittelboom et al. [14] and Jonkers et al. [15]. For successful application in civil engineering  
55 structures, new materials need to satisfy many criteria including affordability, availability, robustness,  
56 durability, performance across a range of exposure environments, chemically inertness and low toxicology.  
57 Superabsorbent polymer (SAP) is a promising class of materials that potentially meets these criteria.

58 Superabsorbent polymers, also known as hydrogels, are cross-linked polymers that have the ability to  
59 absorb a disproportionately large amount of liquid, expanding to form an insoluble gel. A unique  
60 characteristic of SAP is that its swelling rate and capacity can be altered depending on the polymer type and  
61 properties of the liquid including composition, temperature and pressure. For example, the swelling ratio of  
62 SAP in deionised water can be greater than 500 g/g, but it drops to about 10-20 g/g in typical concrete pore  
63 solution. The swollen gel forms a barrier to flow and it gradually releases absorbed water when the  
64 surrounding humidity drops. The main application of SAP is in personal hygiene products (diapers). Other  
65 uses include biomedical (bandages), pharmaceutical (drug delivery), agricultural (soil conditioning), waste  
66 solidification, meat packaging and water blocking tapes for undersea cables [16]. In concrete technology,  
67 research on SAP has mainly focused on its use as an internal curing agent to mitigate autogenous shrinkage  
68 in low w/c mixes [17, 18]. Other proposed applications include rheology control, frost protection [19, 20]  
69 and crack sealing/healing [21-26]. A state-of-the-art report on the application of superabsorbent polymers in  
70 concrete has been published by RILEM [27].

71 The use of SAP as an admixture for self-sealing cracks in cement-based materials was described by  
72 Tsuji et al. [21, 22] and this concept was further explored by Lee et. al. [23, 24] and Snoeck et al. [25, 26]. In  
73 the work of Tsuji et al. [22], mortar specimens with w/c ratio 0.5 and sand/cement ratio 1.0 containing up to  
74 3% vol. of SAP (5% wt. cement) were prepared and mechanically loaded to form a single 0.1mm wide  
75 through crack. The flow rate of water through the crack was monitored for 3 hours. Their result showed that

76 the initial flow rate for mortars containing SAP was 90% lower than that of the control sample and the flow  
77 rate rapidly decreased over the following 3 hours. Using neutron radiography to study water penetration,  
78 Snoeck et al. [25], found that mortars containing SAP had lower capillary absorption in comparison to the  
79 control sample. Snoeck et al. [26] also demonstrated the use of SAP to promote self-healing in microfibre-  
80 reinforced mortars exposed to wet-dry cycles in water. They observed that cracks up to 0.13 mm in width  
81 healed completely by  $\text{CaCO}_3$  precipitation, which led to decrease in permeability and regain in mechanical  
82 properties.

83 The aim of this study is to investigate the feasibility of SAP as an admixture for self-sealing cracks in  
84 concrete. Our focus will be cracks wider than 0.1 mm because they have limited ability to self-heal naturally,  
85 cause leakage and impair the watertightness of concrete. Forty samples containing four types of SAP based  
86 on partially neutralised acrylates or acrylate/acrylamide copolymers at varying dosages were prepared. A  
87 single through-thickness crack of between 0.1 and 0.4 mm width was induced in each specimen, which was  
88 then subjected to a flow of 0.12 wt. % NaCl at hydrostatic pressure gradient of 4 m/m to simulate  
89 groundwater ingress. Flow was monitored continuously to study the effect of SAP type and dosage, and  
90 crack width on healing, and the results were compared against control samples that did not contain SAP. In  
91 addition, an analytical model was developed to predict the fraction of crack sealed as a function of crack  
92 width and SAP particle size, dosage and swelling characteristics. The model was applied to support  
93 experimental results and to provide further insights on factors influencing the efficiency of SAP for crack  
94 sealing.

95

## 96 **2. Crack sealing mechanism**

97 Fig. 1 illustrates the envisaged self-sealing mechanism. When concrete is batched, the mix water  
98 reaches a very high pH (~12.5-13) and ionic concentration (~150-700 mmol/L) within minutes in contact  
99 with cement because of rapid dissolution of the cement compounds releasing ions including  $\text{Ca}^{2+}$ ,  $\text{K}^+$ ,  $\text{Na}^+$ ,  
100  $\text{OH}^-$  and  $\text{SO}_4^{2-}$  [28]. As such, SAP that is added during batching will initially swell at a much reduced

101 capacity compared with SAP in freshwater. Calcium ions in the mix water forms a bidentate complex with  
102 the acrylates of the SAP [29], which further limits its swelling [30, 31]. The initial swelling is also confined  
103 by the mixing and compaction processes. As cement hydrates and concrete self-desiccates, the SAP  
104 gradually releases its absorbed water and shrinks, leaving behind voids of tens to hundreds of microns in size  
105 in the cement paste (Fig. 1a). These voids can be viewed as macro-defects, and so cracks that form during  
106 the service life of the concrete structure are likely to propagate through them (Fig. 1b). The SAP lies dormant  
107 in the microstructure until a crack occurs through the SAP voids, exposing the polymer to the external  
108 environment. When the concrete is then subjected to wetting, ingress of water triggers the SAP to swell again.  
109 External fluids such as precipitation and groundwater have much lower ionic concentration compared to  
110 concrete pore solution and so the re-swelling of SAP will increase significantly. The reduced physical  
111 confinement will also increase the re-swelling capacity of the SAP. The swollen SAP forms a soft gel that  
112 expands beyond the void and into the crack, subsequently slowing down or preventing further flow (Fig. 1c).  
113 In addition to the direct physical blocking effect of the swollen SAP, the reduced crack width and flow rate  
114 may promote autogenous healing of cracks [3-6]. If the concrete is exposed to wetting and drying cycles,  
115 then the delayed released of water by the SAP during drying periods may also assist self-healing. These  
116 effects would help retain the water-tightness of cracked structures. To the best of the authors' knowledge, the  
117 ideas presented here were first described in the paper Lee et al. [23].

118

### 119 **3. Experimental**

#### 120 **3.1 Materials**

121 Two cements were used in this study: a) white Portland cement (CEM I, 52.5 N) and b) Portland  
122 composite cement containing 27% fly ash (CEM II/B-V, 32.5R) complying with BS EN 197-1, from Lafarge.  
123 Their oxide compositions are shown in Table 1. The specific gravity of the CEM I and CEM II cements were  
124 3.04 and 2.92 respectively. The aggregates used in mortar and concrete mixes were quartz sharp sand (< 5  
125 mm) and Thames Valley gravel (< 10mm). Their particle size distribution, specific gravity and water

126 absorption are shown in Table 2. The aggregates were oven-dried at 100°C for 24 hours and cooled to room  
127 temperature prior to use. Deionised water was used as batch water.

128 **Twenty** types of commercially available SAP were obtained, from which four were selected and used  
129 for this study. The rest were rejected mainly because it was deemed that their particle sizes and swelling  
130 properties were inappropriate for this application. The selected polymers were either polyacrylate or  
131 polyacrylate-co-acrylamide. The SAPs are the same polymers denoted as S1, S2, S3 and S5 in an earlier  
132 paper [23]. The SAPs are in a white powder form with particle size ranging from several micrometers up to  
133 500µm. S3 has the largest particle size, followed by S2, S5 and S1. When viewed using an optical  
134 microscope in transmitted light and scanning electron microscope, S1, S2 and S5 appear as smooth, angular  
135 shaped granules with a small amount of convoluted sheets. This is a result of the grinding process after  
136 solution polymerization in their manufacture. S3 has a very rough surface texture and appears to be  
137 agglomerates of smaller particles with high surface area due to the two-step suspension polymerization  
138 manufacturing process. S1 has the smallest particle size. Fig. 2 shows scanning electron micrographs  
139 highlighting the differences in particle size, surface texture and particle shape of the SAPs.

140 The properties of the SAPs including their swelling ratios in deionised water, 0.12 wt.% NaCl, synthetic  
141 shallow groundwater and synthetic pore solution are shown in Table 3. The composition of synthetic  
142 groundwater was based on a relatively concentrated groundwater with ionic strength of 21 mmol/L [37], in  
143 mmol/L: NaHCO<sub>3</sub> (8.2), CaSO<sub>4</sub> (1.04), MgSO<sub>4</sub> (2.08) and CaCl<sub>2</sub> (0.14). The composition of synthetic pore  
144 solution was based on pore solution extracted from a 0.5 w/c ratio cement paste within 30 minutes of mixing  
145 [28], in mmol/L: CaSO<sub>4</sub> (20.6), K<sub>2</sub>SO<sub>4</sub> (163.4), KOH (71.2) and NaOH (73.9). Swelling ratio was measured  
146 using suction filtration. 100 mg of SAP predried at 50°C was immersed in 50 mL of the solution for 60 min  
147 at 20°C. The swollen SAP was then filtered by suction (~0.17 bar) over a pre-saturated filter paper for 5 min  
148 and weighed. The swelling ratio is calculated as the water uptake by mass of dry SAP. The obtained values  
149 are close to those reported in the literature [17, 18, 26, 32].

150

**151 3.2 Samples**

152 Fifteen mixes consisting of neat cement paste, mortar and concrete were prepared. These are divided  
153 into four series and their details are shown in Table 4. Series I and II consist of cement pastes with a target  
154 free w/c ratio of 0.3. Series III and IV consist of mortars (w/c 0.5) and concretes (w/c 0.4) respectively.  
155 Mortars were designed with 50% vol. sand, while the concretes were designed with 65% vol. aggregates at  
156 sand-total aggregate ratio of 0.35. The SAP dosage ( $\alpha$ ) ranged from 0% to 13% by weight of cement. For  
157 Series II and IV, white Portland cement was used as the binder to reduce alkalinity and calcium nitrate  
158 tetrahydrate (analytical grade, Fluka) was added to increase the calcium content of the pore solution. The  
159 purpose of this was to depress the initial swelling of SAP [33, 34] so that a higher SAP dosage was possible.  
160 Furthermore, this increases the reswelling capacity of SAP so that the potential for crack sealing is improved.  
161 The amount of calcium nitrate tetrahydrate added was 4% by weight of cement.

162 Mix design was carried out by absolute volume. Water contents for the mortar and concrete mixes were  
163 corrected for aggregate absorption. Mixes with SAP contained additional batch water to account for the  
164 amount absorbed by the SAP so that the target free w/c ratio is achieved. This was determined by conducting  
165 many trial mixes to measure the additional water required to obtain a mix with similar consistency to the  
166 control mix. Consistency was judged by comparing the spread of the freshly prepared mix on a flow table.  
167 Swelling ratio of the SAP was then measured based on the difference in water content between the mix  
168 containing SAP and the control [35]. The results are shown in Table 4 and it can be seen that the swelling  
169 ratios measured in the fresh mix are close, but lower than the free swelling ratios measured in synthetic pore  
170 solution (Table 1), which is to be expected. The results also show the effect of calcium nitrate in depressing  
171 the swelling ratio. It should be noted here that the physical presence of swollen SAP may influence the  
172 rheology of the fresh mix [47] to the extent that it affects the accuracy of the estimated swelling ratios.  
173 Possibly, a more accurate method for measuring the actual swelling ratio in the cement paste is through  
174 detailed image analysis of BSE images, for example as described in Lee et al. [35] and Justs et al. [48].

175 Batching was done in a pan mixer. Cement, SAP and aggregates were mixed thoroughly for 2 minutes.  
176 Water was then added and mixed for another 3 minutes. In mixes marked with \*, calcium nitrate was first

177 dissolved in batch water before addition. Samples were then cast into cylindrical steel moulds (100Ø × 150  
178 mm) with specially fabricated trapezoid inserts to produce grooves on two opposing sides of the samples for  
179 inducing cracks, as shown in Fig. 3. The moulds were filled and compacted in three equal layers on a  
180 vibrating table. The compacted samples were then covered with plastic sheets and stored in a fog room at  
181 100% RH and ambient temperature (21°C) for 5 days. The hardened samples were then demoulded and  
182 cured for another 9 days in the fog room. The top and bottom of each sample was ground to create a flat  
183 surface. The sample was then sealed cured by wrapping in a generous amount of cling film then placed in  
184 sealed polythene bags and stored at ambient temperature and humidity (21°C, 55% RH) for a further 2 weeks.

185

### 186 **3.3 Inducing crack**

187 A single through-thickness crack was induced at the centre of each sample by tensile splitting using the  
188 loading device shown in Fig. 3b. Pressure was applied through a metal bar placed at the tip of each side  
189 groove of the sample. The applied pressure was gradually increased until a single through crack was  
190 produced. This procedure was very effective because the shape of the sample lends itself to splitting between  
191 the grooves without producing visible broken pieces (Fig. 3c). The distance between the tip of each side  
192 groove i.e. the crack breadth was 30 mm. The cracked sample was then briefly taken apart and reassembled  
193 to ensure that a complete through crack was produced. A silicone rubber seal attached to a thin stainless-steel  
194 plate was fitted into the side grooves of the sample. A set of Perspex strips were then inserted into the side  
195 grooves and the assembled sample was held together using three stainless-steel hose clamps (Fig. 3c). The  
196 width of the crack was adjusted by adjusting the Perspex inserts and clamps. Tightening the Perspex strips  
197 widens the crack, while tightening the hose clamps reduces crack width. A stereomicroscope and image  
198 analysis were used to measure the crack width on six locations on the top and bottom flat surfaces of each  
199 sample, and the results were averaged. An angled light source was used to enhance the contrast of the crack  
200 and to increase the accuracy of the crack width measurement. In total, forty samples with average crack  
201 widths ranging from 0.1 mm to 0.4 mm were prepared in this manner for testing.

202

### 203 3.4 Measuring flow through crack

204 Fig. 4 shows the setup of the flow through crack (FTC) experiment, which was specifically designed to  
205 study transport of fluids in cracked concrete [36]. The ends of the sample were attached to an inlet and an  
206 outlet cell using silicone sealant. These cells were fitted with sensors to monitor the temperature of the inlet  
207 solution, and pH and resistivity of the outlet solution. The inlet cell was connected to a tank containing  
208 0.02M (0.12 wt. %) sodium chloride solution as the permeating medium, positioned to apply a constant 0.6  
209 m head to the sample. This generates a hydraulic gradient of 4 m/m to simulate groundwater seepage in  
210 basements. The flow through the cracked sample was measured every minute using a data logger. Flow was  
211 monitored until it became negligible. A note should be made concerning the choice for the test solution.  
212 Natural groundwater varies greatly in composition since it depends on factors such as aquifer type, mineral  
213 solubility, residence time and temperature. However, the principal ions are calcium, magnesium, sodium,  
214 potassium, sulphate, chloride and bicarbonate [37]. Because of the variability in groundwater composition, a  
215 0.02M NaCl solution was used as a simple substitute for groundwater. This selection was based on our  
216 measurements (Table 3) showing that the swelling ratios of the SAP in 0.02M NaCl are very close to that in  
217 a relatively concentrated groundwater solution.

218

### 219 3.5 Flow through crack containing deposited SAP

220 SAP particles were deposited directly on the crack surface to examine if this will alter crack sealing  
221 compared to samples containing cast-in SAP. Replicate paste sample CP1 was prepared and split into two  
222 halves as described in Section 3.3. The edges of each halve were sealed with duct tape to create a barrier for  
223 ponding. Then, 50 ml distilled water was poured on the crack surface and 25 mg of SAP S1 were sprinkled  
224 and mixed into the pond. The sample was then dried at 50°C for 24 hours to allow the SAP to deposit on to  
225 the crack surface. The SAP concentration on the crack, i.e. the mass of dried SAP exposed per unit crack  
226 area is thus 0.52 mg/cm<sup>2</sup>, which is theoretically equivalent to that of samples containing 5% SAP by weight

227 of cement at w/c ratio of 0.3. The two halves were then reassembled with the rubber seals, Perspex inserts  
228 and clamps, and tested as described in Section 3.3. The sample was labelled as CP1-5S1-dep.

229

### 230 **3.6 Microscopy**

231 At the end of the FTC experiment, samples were examined and imaged with a stereomicroscope to  
232 observe the extent of the crack sealing. The effect of SAP on the microstructure was also examined using  
233 backscattered electron microscopy. The samples were oven-dried at 50°C, trimmed into 40 × 20 × 10 mm  
234 blocks, and vacuum impregnated with a low viscosity fluorescent epoxy resin according to the procedure  
235 described in [38]. The sample surface was then ground using silicon carbide papers of grit sizes 220, 500 and  
236 1200, and diamond polished at 9, 6, 3, 1 and ¼ µm. The polished surface was then carbon coated and  
237 examined with a field-emission scanning electron microscope at 10 keV beam energy.

238

## 239 **4. Results**

### 240 **4.1 Flow-through crack and crack sealing**

#### 241 *4.1.1 General observations*

242 The measured flow rate and cumulative flow over time for all samples are plotted in Figs. 5 to 10. These  
243 are grouped according to sample series and average crack width. The results show that flow rate increased  
244 rapidly and reached a peak value within the first five minutes of measurement. Subsequently, the flow rate  
245 remained relatively constant for a period of time, and then gradually declined to a negligible value. This  
246 seems to be the characteristic of most samples, with or without SAP. The drop in flow rate is due to either  
247 autogenous crack healing or self-sealing from the action of the swollen SAP. The cumulative flow also  
248 showed a relatively consistent trend. Total flow increased rapidly at early stages of the experiment and then  
249 gradually stabilised after the first 24 hours of measurement. Of the forty sets of measurements, four had to be  
250 terminated before complete sealing occurred because the total flow exceeded the 100 L capacity of the test

251 setup. These were the CP1 samples with 0.37 mm crack width (Fig. 8) and the control sample CP2 with 0.3  
252 mm crack width (Fig. 7). For samples containing SAP, all but one gave much lower cumulative flow relative  
253 to the control sample. The exception was CP1-5S1 (Fig. 5b). Overall, the addition of SAP decreased peak  
254 flow rate and cumulative flow by up to 85% and 98% respectively, and sealed the 0.3 mm crack.

#### 255 4.1.2 *Effect of SAP type*

256 Fig. 5 presents the results from Series I, which are pastes containing 4-5% SAP tested at an average  
257 crack width of 0.2 mm. Samples containing S2 (CP1-5S2) and S5 (CP1-4S5) showed significantly lower  
258 peak flow rates and cumulative flow relative to the control. For CP1-5S2, the reduction was 55% and 80%  
259 for peak flow rate and cumulative flow respectively. For CP1-4S5, tests were carried out on two replicate  
260 samples and the results show a consistent reduction in peak flow rate by 75-85%, and reduction in  
261 cumulative flow by 75-80% compared to the control. Samples containing S3 (CP1-5S3) gave a slightly  
262 higher peak flow rate, but the total flow was 25% lower than the control. However, the total flow for samples  
263 containing S1 (CP1-5S1) was 80% higher than the control. These results suggest that S2 and S5 are more  
264 effective than S1 and S3 for sealing cracks. Therefore, a greater emphasis was placed on the use of S2 and  
265 S5 in subsequent experiments.

#### 266 4.1.3 *Effect of calcium nitrate and SAP dosage*

267 As stated in Section 3.2, selected mixes contained dissolved calcium nitrate to depress the initial  
268 swelling of the SAP. The purpose of this was to enable higher dosages of SAP in the mix, to increase the re-  
269 swelling capacity of the SAP and thereby its potential for crack sealing. With this approach, we were able to  
270 cast samples with up to 13% SAP by weight of cement. The FTC data for samples containing 13% S2 and 8%  
271 S5 are plotted in Fig. 6. Compared to the data from Series I (Fig. 5), the results show the higher SAP dosage  
272 produced a more rapid crack sealing and lower cumulative flow. The total flow at the end of the experiment  
273 for CP2-13S2\* and CP2-8S5\* was only around 0.6 L compared to 6.2 L for CP2\* (90% reduction) and 27.3  
274 L for the control CP2 (98% reduction). This is clearly a result of the greater amount of SAP that is exposed  
275 by the crack. It should be clarified here that this is not due to densification of the pore structure from internal

276 curing because flow occurs via the induced crack, rather than the pore structure of the sample. It is also  
277 interesting to note that the addition of calcium nitrate decreased the flow rate and cumulative flow of the  
278 control sample. This can be seen by comparing the data from CP2\* to that of CP2 in Fig. 6. A possible  
279 explanation for this is that the higher calcium concentration in CP2\* led to a more rapid autogenous crack  
280 healing resulting from more precipitation of calcium carbonate and possibly calcium hydroxide. To the best  
281 of our knowledge, this enhanced self-healing brought by calcium nitrate has not been reported before.

#### 282 4.1.4 Effect of crack width

283 In the next set of experiments, replicate samples from Series II were subjected to a larger crack width of  
284 0.3 mm and put through the FTC test. Comparing the results in Fig 7 to Fig 6 shows that the flow rates and  
285 cumulative flow for all samples increased significantly with increase in crack width, which is to be expected.  
286 Nevertheless, crack sealing with SAP remained effective. The flow rates for CP2-8S5\* and CP2-13S2\*  
287 reduced to negligible values after 200 minutes. In contrast, the flow rate for CP2 remained very high at about  
288 2500 mm<sup>3</sup>/s throughout the experiment. Unfortunately, the measurement for CP2 had to be stopped after 700  
289 minutes when its total flow exceeded the 100 L capacity of the test setup. Judging from the trend of the  
290 collected data, the final cumulative flow for CP2 would have exceeded 100 L by several times. In contrast,  
291 the final cumulative flow for CP2-8S5\* and CP2-13S2\* were only 4.9 L and 2.3 L respectively, a reduction  
292 of at least 95% and 98%. The results also show that the presence of SAP was able to decrease flow rate and  
293 total flow beyond the levels achieved by adding calcium nitrate alone (CP2\*). These results demonstrate the  
294 effectiveness of the combined action of calcium nitrate and SAP in sealing cracks.

295 In another set of experiments, replicate samples from Series I and Series II were subjected to crack  
296 widths ranging from 0.1-0.4 mm. Fig. 8 shows the measured peak flow rate against crack width and the  
297 results are compared against the Hagen-Poiseuille equation for steady-state laminar flow between parallel  
298 plates, given by  $Q = bw^3\Delta P/12\mu L$ , where  $Q$ ,  $b$ ,  $w$ ,  $\Delta P$ ,  $\mu$ , and  $L$  are the flow rate, crack breadth, crack width,  
299 differential pressure, fluid viscosity and length of the flow path. Data from samples with SAP deposited  
300 directly onto the crack surface (CP1-5S1-dep) are also plotted on Fig. 8. The results show that the measured  
301 flow rates increased significantly with crack width and follow approximately the trend of the Hagen-

302 Poiseuille equation. However, the measured flow rates are significantly lower than theoretical values. This is  
 303 expected because the actual geometry, tortuosity and surface roughness of real cracks have a major influence  
 304 on flow, but these are not captured in the Poiseuille equation. Flow rates for the control, sample with cast-in  
 305 SAP and sample with deposited SAP are lower than the theoretical values by an average of 47%, 70% and 95%  
 306 respectively. Overall, the results show that SAP is effective in decreasing peak flow rates for a range of crack  
 307 widths. It is also evident that a greater reduction in peak flow rate was achieved when SAP was deposited  
 308 onto the crack compared to cast-in SAP. A possible explanation is that the SAP deposited on the crack  
 309 surface has not been mixed with the pore solution and is not physically confined by the SAP void along the  
 310 crack surface.

#### 311 4.1.5 Crack sealing in mortars and concretes

312 Results from mortars (Series III) and concretes (Series IV) are presented in Fig. 9 and 10 respectively.  
 313 For both sets of results, the FTC experiment was carried out on samples with 0.3 mm average crack width.  
 314 Similar to paste samples, the mortars and concretes containing SAP showed more rapid crack sealing and  
 315 significantly lower flow rates and cumulative flow relative to the control. The mortars (M-5S1 & M-5S2)  
 316 gave 25-50% lower peak flow rates and 80-88% lower cumulative flow compared to the control. S2 was  
 317 more effective than S1, consistent with results from Series I. The concretes (C-13S2\* & C-8S5\*) gave very  
 318 similar peak flow rates to the control, but they dropped rapidly to negligible values after 13 hours of  
 319 measurement compared to 134 hours for the control. Consequently, the total flow through C-13S2\* & C-  
 320 8S5\* are less than 5% of the control.

#### 321 4.1.6 Effect of SAP dosage on cumulative flow and time to crack sealing

322 Fig. 11 shows the effect of SAP dosage on the time to reach a negligible flow rate and on the cumulative  
 323 flow. The results are compiled from data taken on all samples from Series I-IV with crack widths of 0.2 mm  
 324 and 0.3 mm. A 'negligible' flow rate is arbitrarily defined here as  $10 \text{ mm}^3/\text{s}$  ( $= 0.33 \text{ mm}^3/\text{s}$  per mm crack  
 325 breadth). Please note the logarithmic scale on the Y-axis. The time to crack sealing ranged from 1 hour to  
 326 about 5 days. Overall, the figure shows that increasing SAP dosage has a huge effect on accelerating crack

327 sealing and decreasing the total flow through the crack. A difference of more than a factor of 10 can be  
328 observed. The figure also suggests that reductions in time to crack sealing and cumulative flow were  
329 insignificant when the SAP dosage was above 8% (for crack widths of 0.2-0.3 mm).

330

#### 331 **4.2 Visual assessment of crack sealing**

332 Samples were examined with a stereomicroscope immediately after the FTC experiment. Typical  
333 images of the upstream and downstream faces of a sample containing SAP are shown in Fig. 12. The  
334 upstream face was in constant contact with the test solution, so it can be seen that the swollen SAP forms a  
335 transparent gel that fills a significant portion of the crack (Fig. 12a). In contrast, the downstream face is dry  
336 because flow has stopped by the end of the FTC experiment due to crack sealing. Therefore, the SAP  
337 particles near the downstream face are not swollen and the crack is clearly visible (Fig 12c). The upstream  
338 face was observed again after the sample was dried at room temperature for 24 hours. It can be seen that the  
339 swollen SAP has shrunk and the crack is clearly visible again (Fig. 12b). Figs. 12d & 12e show area  
340 matching views of the internal crack surface before and after wetting with the test solution. Remnants of the  
341 dry SAP can be seen residing in their voids. When wetted, the SAP swells beyond its original void and  
342 expand into the crack space. These observations correspond well with the FTC results and support the  
343 envisaged crack sealing mechanism described in Section 2 and Fig. 1. It is also worth noting that no  
344 significant deposits were observed on the sealed cracks, indicating that the crack is not blocked when the  
345 sample is dry.

346

#### 347 **4.3 Microstructure of samples containing SAP**

348 Fig. 13 shows a selection of micrographs from BSE imaging to highlight the size, shape and distribution  
349 of the SAP particles and voids, and their effect on the microstructure of cement-based materials. It can be  
350 seen that the SAP voids are isolated and well-distributed in the paste. Their size ranges from  $\sim 10\mu\text{m}$  to over

351 500 $\mu$ m, depending on the initial size of the dry SAP and the amount of swelling in the paste. These can be  
352 easily differentiated from entrapped air voids, which are spherical and empty. The boundary of the SAP void  
353 tends to follow the shape of the collapsed SAP particle, which may appear as solid, porous, cellular or  
354 narrow ring-shaped particle. The appearance of the SAP depends on the original particle shape, how it is  
355 sectioned during sample preparation for microscopy, and the way in which it is restrained by the surrounding  
356 cement paste when it dries.

357 Samples containing S1, S2 and S5 tend to show a gap between the SAP and cement paste due to  
358 shrinkage of the polymer (Fig. 13 a, c, d). However, this feature is not seen in samples containing S3 (Fig.  
359 13b). This suggests that the rough texture and large surface area of S3 helps to strengthen its adhesion with  
360 the cement paste (Fig. 2c). Occasionally, the SAP voids appear to contain small cement grains that have  
361 subsequently reacted to form hydration products within the water reservoirs of S3. The strong bond between  
362 S3 and cement paste will interfere with its re-swelling capacity, and this would affect its ability to seal cracks  
363 as observed in the FTC results shown in Fig. 5.

364 The cement paste surrounding SAP exhibits a highly variable microstructure, reminiscent of the  
365 aggregate-paste “interfacial-transition zone” and air void-paste interface [39-41]. It contains less cement  
366 particles compared to the bulk paste region farther away due to the disrupted packing of the cement grains. It  
367 also tends to be very porous and occasionally contains large calcium hydroxide deposits. These features can  
368 be attributed to the high water content on the surface of swollen SAP or possibly the early release of  
369 absorbed water into the surrounding paste. Shrinkage of the SAP when it dries may also lead to cracking of  
370 the surrounding cement paste. Samples from Series II and IV that contain high SAP dosages show very  
371 closely spaced SAP voids (Fig. 13c). The ratio of SAP void area to SAP particle is also smaller because of  
372 the depressed swelling as a result of the calcium nitrate addition. In mortars and concrete samples, it can be  
373 seen that the SAP voids are of the size of sand grains and they can span between aggregate particles.

374

#### 375 4.4 Effect of high SAP dosage on compressive strength

376 It is fairly well-established that the use of SAP often results in a decrease in compressive strength, even  
377 at low SAP dosages of less than 1% by mass of cement, see for examples Kovler [49] and Hasholt et al. [50].  
378 To examine the effect of the relatively high SAP dosages used in this study on compressive strength, selected  
379 mixes of cement paste, mortar and concrete with and without SAP were prepared and 100 mm cube samples  
380 were cast in three replicates following the procedure described in Section 3.2. The cubes were demoulded  
381 after one day and then cured in water at 20°C for 28 days prior to compressive strength testing. The emphasis  
382 was on polymer S2 since this particular SAP was found to very effective for crack sealing.

383 The results of the 28-day compressive strength testing are shown in Table 5. For the control samples, it  
384 can be seen that increasing w/c ratio decreases strength. As expected, all specimens containing SAP achieved  
385 compressive strengths much lower than their respective controls. The level of strength reduction for the  
386 samples tested ranged between 80% and 87%. This is due to the high volume of SAP voids in the  
387 microstructure as can be seen in Fig. 13. An interesting observation is that the strength of mixes containing  
388 13% SAP was not significantly lower compared to that of mixes containing 5% SAP. In fact, the amount of  
389 strength loss per 1% added SAP decreased from ~17% (for 5% S2) to ~7% (for 13% S2). This is due to the  
390 effect of the added calcium nitrate which decreases the swelling of the SAP and thus controls the volume of  
391 SAP voids in the mix containing 13% SAP. Therefore, depressing the initial swelling of SAP helps to reduce  
392 its detrimental effect on strength.

393

#### 394 5. Modelling

395 In this section, a mathematical model is developed and applied to better understand the factors  
396 influencing crack sealing with SAP. Here, we attempt to estimate the volume fraction of crack filled ( $\psi$ ) as a  
397 function of its width ( $w$ ), dry SAP particle size ( $d_o$ ), SAP dosage ( $\alpha$ , mass fraction of cement), initial  
398 swelling ratio in cement paste ( $S_1$ ) and the subsequent re-swelling ratio ( $S_2$ ) triggered by ingress of external  
399 fluids via the crack. This will be achieved by first estimating the mass of SAP exposed in a crack, and then

400 calculating the swollen gel volume that intrudes the crack, taking account of the volume of the initial SAP  
 401 voids. For simplicity, we represent the dry SAP particles as mono-sized spheres of diameter  $d_o$  dispersed in a  
 402 random, uniform and isotropic manner in the cement paste. When batched in concrete, each SAP particle  
 403 swells to a sphere and leaves a void of diameter  $d_l$  when it dries and shrinks.

404 The crack is modelled as a flat plane that randomly intersects the cement paste matrix. If the crack  
 405 propagates through an SAP void, then the SAP particle in the void is ‘exposed’ to external wetting. The mass  
 406 of SAP exposed per area of crack,  $m_A$  is given by:

$$m_A = N_A \times m_o \quad (1)$$

407 Where  $N_A$  is the number of SAP particles per area of crack intersected by the random plane and  $m_o$  is the  
 408 mass of one dry SAP particle. Using stereology,  $N_A = N_V d_l$ , where  $N_V$  is the number of SAP particles per  
 409 volume of the sample [42, 43]. From mix design,  $N_V = (\alpha C) / m_o$ , where  $C$  is the cement content ( $\text{kg}/\text{m}^3$ ).

410 By assuming that the volume of a swollen SAP equals the sum of volumes of the dry SAP and absorbed  
 411 solution, the diameter of an SAP void  $d_l$  can be related to the diameter of a dry SAP particle  $d_o$  via:

$$d_l = d_o \left( S_1 \frac{\rho_{SAP}}{\rho_{abs}} + 1 \right)^{\frac{1}{3}} \quad (2)$$

412 Where  $\rho_{SAP}$  and  $\rho_{abs}$  are the densities of the dry SAP and absorbed solution respectively. Substituting (2) and  
 413 the above expressions into Eq. (1) leads to the following equation:

$$m_A = \alpha C d_o \left( S_1 \frac{\rho_{SAP}}{\rho_{abs}} + 1 \right)^{\frac{1}{3}} \quad (3)$$

414 When external fluids percolate through the crack, the SAP will absorb an amount equal to  $S_2 m_A$ , causing  
 415 each SAP particle to swell beyond its void and into the crack. The volume fraction of crack filled  $\psi$  is given  
 416 by:

$$\psi = \frac{\text{Swollen SAP vol.} - \text{SAP void vol.}}{\text{Crack vol.}} = \frac{m_A \left( \frac{1}{\rho_{SAP}} + \frac{S_2}{\rho_{abs}} \right) - m_A \left( \frac{1}{\rho_{SAP}} + \frac{S_1}{\rho_{abs}} \right)}{w} = \frac{m_A (S_2 - S_1)}{w \rho_{abs}} \quad (4)$$

417 Inserting Eq. (3) into Eq. (4) and rearranging gives:

$$\psi = \frac{\alpha C d_o (S_2 - S_1)}{w \rho_{abs}} \left( S_1 \frac{\rho_{SAP}}{\rho_{abs}} + 1 \right)^{\frac{1}{3}} \quad (5)$$

418 Fig. 14a shows the results of the fraction of crack filled as a function of crack width ( $w$ ) for various  
 419 dosages of SAP ( $\alpha$ , wt. % of cement). The simulations were carried out on a sample with 0.3 w/c ratio,  
 420 assuming that  $S_1 = 10$  g/g,  $S_2 = 75$  g/g and  $d_o = 100$   $\mu\text{m}$ . The value for  $S_1$  was chosen based on the measured  
 421 swelling ratio in cement paste (Table 4), while the value for  $S_2$  was chosen based on the free swelling ratio  
 422 measured in 0.12 wt. % NaCl solution (Table 3), which is the solution used in the FTC experiments. The  
 423 densities of the dry SAP ( $\rho_{SAP}$ ) and absorbed solution ( $\rho_{SAP}$ ) were taken as 1660 kg/m<sup>3</sup> [16] and 1000 kg/m<sup>3</sup>  
 424 respectively. The results show that the fraction of crack filled increased with increase in SAP dosage with  
 425 decrease in crack width, as expected. The simulations also show that an SAP dosage of 1% by weight of  
 426 cement would fully seal a crack of 0.2 mm and that a dosage of 5% by weight of cement would seal a crack  
 427 of 0.7 mm.

428 Further simulations were carried out to establish the main factors that influence crack filling and explore  
 429 methods to enhance the effectiveness of SAP. A selection of the additional simulations is shown in Figs. 14b,  
 430 14c and 14d. The sensitivity analysis shows that the crack filling performance can be enhanced greatly by  
 431 increasing swelling ratio  $S_2$ . For example, Fig. 14c shows that when  $S_2$  is doubled to 150 g/g from 75 g/g, the  
 432 crack width filled by an SAP dosage of 1% increases to 0.5 mm. This is because of the increased gel volume  
 433 available to fill the crack. A similar effect can be achieved by doubling the SAP particle size  $d_o$  from 100  $\mu\text{m}$   
 434 to 200  $\mu\text{m}$  (Fig. 14d) while maintaining the dosage. This is because a larger particle size increases the mass  
 435 of SAP exposed in a crack as shown in Eq. 3. In practice, a larger SAP size would also increase the size of  
 436 the swollen gel and therefore its ability to bridge cracks. In our experiments, polymer S1 has the smallest  
 437 particle size (Fig. 2) and was the least effective in terms of crack sealing. This observation seems consistent  
 438 with the model. Limiting the initial swelling  $S_1$  is also beneficial. For example, Fig. 14b shows improved  
 439 crack sealing performance when the initial swelling  $S_1$  is reduced from 10 g/g to 5 g/g. However, the  
 440 improvement is small relative to that achieved by changing  $S_2$  or  $d_o$ . This is because of opposing effects

441 when  $S_I$  is depressed. On the one hand, it increases the contrast ( $S_2 - S_I$ ) and this improves crack sealing. On  
442 the other hand, it decreases the size of the SAP void and therefore lowers the probability of the SAP particles  
443 being intersected by a random crack.

444

## 445 **6. Discussion**

446 The reduction of flow with time in cracked concrete, i.e. autogenous healing, occurs as a result of  
447 several physical and chemical processes. For example, the crack could be blocked by loose fine particles  
448 dislodged from the fractured surface. A major contributing factor is that material upstream are weakened and  
449 eroded by leaching, and then carried by the percolating water and deposited in constrictions further  
450 downstream [36]. Other possibly contributing processes include swelling of the cement paste, carbonation of  
451 hydration products forming  $\text{CaCO}_3$  precipitates, dissolution and re-precipitation of calcium hydroxide within  
452 the crack, and hydration of exposed unreacted cement particles forming new products that fill the crack [3, 4,  
453 44]. In samples containing SAP, the swollen SAP forms a soft gel that expands into the crack. This “gel  
454 blocking” effect further reduces the rate and total flow, and the time to reach negligible flow compared to the  
455 control as seen in the FTC experiments. The swollen SAP is also expected to enhance autogenous healing by  
456 narrowing the crack pathway and physically trapping fine particulates or by acting as nucleation sites to  
457 encourage precipitation of solid products. However, the significance of this is unclear and further study is  
458 required. It is worth noting that no significant amounts of deposits were seen in the healed cracks, suggesting  
459 that healing is primarily due to physical blocking by swollen SAP. This is in contrast to the work of Snoeck  
460 et al. [26] who observed healed cracks were filled with  $\text{CaCO}_3$  deposits for samples that were continuously  
461 submerged or exposed to wetting and drying. The difference is probably due to the fact that our samples  
462 contained wider cracks and were not exposed to wet/dry cycles which facilitate carbonation and precipitation.

463 It is interesting to note that swelling of unconfined SAP in solution occurs instantaneously. However,  
464 when cast in concrete, the re-swelling of SAP exposed in a crack seems to occur at a much slower rate. This  
465 can be deduced from the observation that flow does not stop abruptly during the FTC experiments. Instead, it

466 declines gradually, even in samples where the SAP dosage is estimated to be way above the amount required  
467 to completely fill the crack (Fig. 14a). In contrast, crack filling and the decrease in flow rate occurs very  
468 rapidly if SAP is deposited on the crack surface (Section 3.5) or placed in a model crack made of two parallel  
469 glass slides as shown in an earlier study [23]. There are several possible reasons for this. One is that the re-  
470 swelling of cast-in SAP is much smaller than expected from the free swelling measured in solution. This may  
471 be due to the fact that the composition of fluid percolating the crack is not constant, but increases as a result  
472 of leaching of dissolvable species from the cement paste. This would also depend on the flow rate and  
473 residence time. Swelling may also be reduced because of confinement, either by the local geometry of the  
474 SAP void and crack, or by the bond between SAP and cement paste resulting from the rough surface texture  
475 of the polymer and growth of hydration products into the SAP void (as seen for S3, Fig. 13b).

476 Another reason for the delayed crack sealing is because calcium ions form a bidentate complex with the  
477 acrylates of the SAP that limits its initial swelling [29-31] when SAP is cast in concrete. However,  
478 monovalent cations (e.g.  $\text{Na}^+$ ) that are present in the fluid percolating the crack will gradually displace the  
479  $\text{Ca}^{2+}$  complexes from the acrylate chain, and this leads to a recovery in swelling and improved absorption  
480 capacity. In another study, we investigated the swelling of SAP that was initially immersed in a calcium  
481 bearing solution, dried and then exposed to several cycles of NaCl solution [45]. It was observed that the  
482 swelling in NaCl was initially depressed, but gradually increases with repeated exposure to NaCl. Certain  
483 types of SAP recover much faster and are able to achieve a complete recovery of the swelling. This shows  
484 that much of the restraint on swelling caused by the complexes can be removed when enough monovalent  
485 ions are available to displace  $\text{Ca}^{2+}$  from the acrylate chains.

486 The model developed in this study provides a useful tool for predicting crack-sealing with SAP and  
487 understanding factors that influence it. However, several simplifying assumptions were made in its  
488 development. For example, SAP particles were assumed to be mono-sized spherical particles and the crack  
489 was approximated as a flat plane of equal width through the cement paste. An actual crack may propagate  
490 through aggregate particles or around them, depending on the relative stiffness and strength of the aggregate,  
491 cement paste and the interface between them. If the crack propagates through aggregate particles, then the

492 number of exposed SAP would be smaller than predicted. In reality, cracks are more likely to propagate  
493 through the SAP voids since they are a weak phase in the composite. Therefore, the number of SAP exposed  
494 in a real crack would be higher than that assumed in the model. Another assumption is that the crack needs to  
495 be completely filled with swollen SAP to stop flow, but this may not be necessary. As seen in Section 4.2  
496 and Fig. 12, swelling of the SAP near the upstream wetting face is sufficient to seal the crack and stop flow.  
497 It is also not certain what the re-swelling ratio of the SAP is in a real crack, this was assumed to be equal to  
498 the free swelling value measured in solution. It would be interesting to carry out further tests to examine  
499 these assumptions.

500 At present, the relatively high dosage of SAP required for crack sealing will probably limit its practical  
501 application due to cost implications and the undesirable effect on strength. However, the SAP types used in  
502 this study are by no means ideal for the purpose of crack sealing. For example, spherical SAP could help  
503 reduce its adverse effects on strength [18]. There is much scope for optimisation since the physical and  
504 chemical properties of SAP can be tailored to influence swelling behaviour. For example, the degree of  
505 cross-linking and its distribution in the polymer can be altered to decrease constraint and elasticity, thereby  
506 increasing swelling and to produce a more deformable gel that fills cracks more effectively.

507 Modeling suggests that increasing the swelling contrast  $S_2-S_1$  and increasing the particle size of SAP will  
508 enhance its performance for crack sealing. These effectively increase the amount of SAP exposed in a crack  
509 and the available gel volume to block the crack. Limiting the initial swelling  $S_1$  would also be good from the  
510 point of view of reducing total porosity and therefore the effect of SAP on strength. This was observed in the  
511 strength results presented in Section 4.4 for mixes containing calcium nitrate, which was added to depress  
512 the initial swelling of the SAP. The model also suggests that cracks much larger than 0.4 mm can be self-  
513 sealed with SAP, assuming that the re-swelling of SAP in the crack is similar to the unconfined swelling in  
514 solution. Therefore, it would be interesting to test samples with crack widths wider than 0.4 mm in future. If  
515 true, then this would have the potential of reducing the stringent crack width requirement for water-retaining  
516 concrete structures, leading to thinner sections or less steel reinforcement. Stopping flow through large  
517 cracks would enhance overall durability in particular delaying the onset of reinforcement corrosion.

518 More studies are required to examine the longevity of the crack sealing, its effectiveness in real  
519 exposure environments and the influence of SAP on properties of concrete, most notably mechanical  
520 properties and long-term durability. Studies have shown that the swelling of SAP remains fairly consistent  
521 when exposed to wetting and drying cycles [23]. This indicates that SAP can re-swallow after drying with no  
522 apparent deterioration in swelling capacity, which is obviously desirable for crack sealing application.  
523 Another attraction of SAP is that the swollen gel is non-rigid and so it should potentially accommodate some  
524 crack movements, which would otherwise re-open cracks and disrupt autogenous healing based on solid  
525 precipitation. Whether or not SAP remains effective for sealing cracks subjected to higher hydraulic  
526 gradients or other types of percolating fluids remains to be seen. A high percolating fluid pressure may  
527 decrease the effectiveness of the SAP swelling and crack sealing, or wash out the exposed SAP. Another  
528 concern is that repeated swelling of SAP in concrete subjected to wetting and drying may have damaging  
529 effects to the SAP. Also, in saturated concrete exposed to a cold environment, the freezing of wet SAP may  
530 cause problems. It would also be interesting to carry out tests on mixes containing lower SAP dosages and  
531 with addition of calcium nitrate (to depress initial swelling). This is to establish if crack sealing remains  
532 effective at lower SAP dosages and to what extent the reduced initial swelling can help to limit strength loss.  
533 All of these issues merit further investigation.

534

## 535 **7. Conclusions**

536 The feasibility of superabsorbent polymers (SAP) as admixtures to impart the ability to self-seal cracks in  
537 concrete was demonstrated via a series of mass transport experiments, microscopy and modelling. Cement  
538 paste, mortar and concrete samples containing four SAP types at varying dosages and through-thickness  
539 crack widths between 0.1 and 0.4 mm were tested. The flow rate and cumulative flow of 0.12 wt. % NaCl  
540 were measured over time to simulate groundwater seepage in basements. The main conclusions are:

- 541 a) SAP is effective in enhancing crack sealing. The peak flow rate and cumulative flow through samples  
542 containing cast-in SAP decreased by up to 85% and 98% respectively, relative to control samples with

- 543 similar crack widths. This lead to the sealing of a 0.3mm crack. Further research is required to verify its  
544 viability for sealing wider cracks.
- 545 b) Time to reach negligible flow ( $< 0.33 \text{ mm}^3/\text{s}$  per mm crack breadth) ranged from 1 hour for samples  
546 containing SAP to about 5 days for the control samples. Increasing the SAP dosage accelerates sealing  
547 and decreases total flow through the crack significantly. Improvements of more than a factor of ten were  
548 observed.
- 549 c) Addition of calcium nitrate depresses the initial swelling ( $S_1$ ) of SAP. This is beneficial as it allows a  
550 higher SAP dosage, increases the swelling contrast ( $S_2 - S_1$ ) and decreases the size of SAP voids in  
551 cement paste, therefore reducing its impact on strength. Calcium nitrate also enhanced autogenous  
552 healing of the control samples.
- 553 d) Microscopic examination following the end of flow through crack experiments revealed that SAP  
554 particles near the downstream face are dry while those near the upstream face swell to form a soft gel  
555 that fills the SAP void and crack. This is in agreement with the proposed crack sealing mechanism.
- 556 e) BSE imaging shows the SAP particles and voids ( $\sim 10\text{-}500\mu\text{m}$ ) are well-distributed in the cement paste.  
557 The paste surrounding SAP resembles that of the aggregate-paste 'interfacial transition zone' in that it is  
558 highly variable, contains less cement and higher porosity compared to the bulk paste. It also contains  
559 large calcium hydroxide deposits. These features are due to the disrupted particle packing, high water  
560 content on the surface of SAP and possibly the early release of absorbed water into the surrounding  
561 paste. SAP with rough surface texture bonds very well with cement paste, which interferes with its re-  
562 swelling capacity and ability to seal cracks.
- 563 f) At present, the relatively high dosage of SAP used in this study will limit practical applications due to  
564 the high costs involved and the undesirable effect on strength. For example, the addition of 5-13% SAP  
565 by weight of cement was found to reduce compressive strength by 80-87%. Further work is necessary to  
566 establish the feasibility of crack sealing at lower SAP dosages and to develop means to limit strength  
567 loss, for example by depressing initial swelling via the addition of calcium-based salts.

568 g) Analytical modelling shows that the effectiveness of SAP for crack filling can be enhanced by  
569 increasing the re-swelling ratio ( $S_2$ ) and dry particle size ( $d_o$ ), and depressing the initial swelling ratio  
570 ( $S_1$ ). These effectively increase the amount of SAP exposed in a crack and the gel volume that fills the  
571 crack. Simulations based on properties of the SAP used in this study show that an SAP dosage of 1% by  
572 weight of cement would seal a 0.2 mm crack, and an SAP dosage of 5% would seal a 0.7 mm crack,  
573 assuming the swelling of SAP in a crack is similar to unconfined swelling in synthetic solutions.

574

#### 575 **Acknowledgement**

576 We would like to thank Andrew Morris for his assistance with sample preparation and BASF, Evonik and  
577 ETi for provision of SAP samples. This project was supported by an EPSRC Doctoral Training Award held  
578 by H.X.D. Lee.

#### 579 **References:**

- 580 [1] Concrete Society (2010), Technical Report 22: Non-structural cracks in concrete, 4<sup>th</sup> Edition,  
581 Camberley.
- 582 [2] Concrete Society (1995), Technical Report 44: The relevance of cracking in concrete corrosion of  
583 reinforcement, Camberley.
- 584 [3] C. A. Clear (1985), The effect of autogenous healing upon leakage of water through cracks in concrete,  
585 Cement and Concrete Association, Technical Report 559, Wexham Springs, Slough, UK
- 586 [4] N. Hearn (1998), Self-sealing, autogenous healing and continued hydration: What is the difference?  
587 Mater. Struct., 31, 8, 563-567.
- 588 [5] C. Edvardsen (1999), Water permeability and autogenous healing of cracks in concrete, ACI Mater. J.,  
589 96, 4, 448-454
- 590 [6] Y. Yang, M.D. Lepech, E-H. Yang, V.C. Li (2009), Autogenous healing of engineered cementitious  
591 composites under wet-dry cycles, Cem Concr Res, 39, 382-390

- 592 [7] ACI 224R-01 (2001), Control of cracking in concrete structures, American Concrete Institute, Detroit.
- 593 [8] EN 1992-3:2006, Eurocode 2: Design of concrete structures. Part 3: Liquid retaining and containing  
594 structures, European Committee for Standardisation, Brussels.
- 595 [9] ACI 212.3R-10 (2010), Report on Chemical Admixtures for Concrete, American Concrete Institute,  
596 Detroit, 46-50
- 597 [10] Concrete Society (2013), The influence of integral water-resisting admixtures on the durability of  
598 concrete, CS 174, Camberley.
- 599 [11] S. R. White, N. R. Sottos, P. H. Geubelle, J. S. Moore, M. R. Kessler, S. R. Sriram, E. N. Brown, S.  
600 Viswanathan (2001), Autonomic healing of polymer composites, *Nature*, 409, 6822, 794-797
- 601 [12] V.C. Li, Y.M. Lim, Y.W. Chan, (1998), Feasibility study of a passive smart self-healing cementitious  
602 composite, *Compos. Part-B Eng.*, 29, 6, 819-827
- 603 [13] C. M. Dry, (2000), Three designs for the internal release of sealants, adhesives, and waterproofing  
604 chemicals into concrete to reduce permeability, *Cem. Concr. Res.*, **30**, 12, 1969-1977
- 605 [14] K. Van Tittelboom, N. De Belie, D. Muynck, W. Verstraete (2010), Use of bacterial to repair cracks in  
606 concrete, *Cem. Concr. Res.*, 40, 1, 157-166.
- 607 [15] H.M. Jonkers, A. Thijssen, G. Muyzer, O. Copuroglu, E. Schlangen (2010), Application of bacteria as  
608 self-healing agent for the development of sustainable concrete, *Ecological Engineering*, 36, 2, 230-235.
- 609 [16] F. Buchholz, A. Graham, (1998), Modern superabsorbent polymer technology. John Wiley & Sons
- 610 [17] O.M. Jensen, P.F. Hansen (2001), Water-entrained cement-based materials I. Principles and theoretical  
611 background. *Cem Concr Res* , 31 (4), 647-654.
- 612 [18] O.M. Jensen, P.F. Hansen (2002), Water-entrained cement-based materials II. Experimental  
613 observations. *Cem Concr Res*, 32 (6), 973-978.
- 614 [19] S. Mönnig, P. Lura (2007), Superabsorbent polymers – An additive to increase freeze-thaw resistance  
615 of high strength concrete, *Adv Const Mater Part V*, 351-358

- 616 [20] S. Laustsen, M. T. Hasholt, O.M. Jensen (2015), Void structure of concrete with superabsorbent  
617 polymers and its relation to frost resistance of concrete, *Mater. Struct.*, 48, 357-368.
- 618 [21] M. Tsuji, A. Okuyama, K. Enoki, S. Suksawang (1998), Development of new concrete admixture  
619 preventing from leakage of water through cracks, *JCA Proc. of Cement & Concrete*, 52, 418-423
- 620 [22] M. Tsuji, K. Shitama, D. Isobe (1999), Basic studies on simplified curing technique and prevention of  
621 initial cracking and leakage of water through cracks of concrete by applying superabsorbent polymers  
622 as a new concrete admixture, *Journal of the Society of Materials Science, Japan*, 48, 1308-1315
- 623 [23] H.X.D. Lee, H.S. Wong, N.R. Buenfeld (2010), The potential of superabsorbent polymer for self-  
624 sealing cracks in concrete, *Adv Appl Ceram*, 5, 296-302.
- 625 [24] H.X.D. Lee, H.S. Wong, N.R. Buenfeld, (2010), Self-sealing concrete using superabsorbent polymers,  
626 International RILEM Conference on Use of Superabsorbent Polymers and other New Additives in  
627 Concrete, RILEM Publications SARL, 171-178.
- 628 [25] D. Snoeck, S. Steuperaert, K. Van Tittelboom, P. Dubruel, N. De Belie (2012), Visualization of water  
629 penetration in cementitious materials with superabsorbent polymers by means of neutron radiography,  
630 *Cem. Concr. Res.*, 42, 1113-1121
- 631 [26] D. Snoeck, K. Van Tittelboom, S. Steuperert, P. Dubruel, N. De Belie (2014), Self-healing  
632 cementitious materials by the combination of microfibers and superabsorbent polymers, *J. Intell. Mater.*  
633 *Sys. Struct.*, 25, 1, 13-24.
- 634 [27] RILEM TC 225-SAP (2012), Application of superabsorbent polymers (SAP) in concrete construction,  
635 V. Mechtcherine & H.W. Reinhardt (Editors), State-of-the-art report, Springer.
- 636 [28] E. Gartner, F. Tang and S. Weiss, (1985), Saturation factors for calcium hydroxide and calcium  
637 sulfates in fresh Portland cement pastes, *J. Am. Ceram. Soc.*, 68, 12, 667-673

- 638 [29] C. Y. Rha, J. W. Seong, C. E. Kim, S. K. Lee and W. K. Kim, (1999), Properties and interaction of  
639 cement with polymer in the hardened cement pastes added absorbent polymer, *J. Mater. Sci.*, 34, 19,  
640 4653-4659
- 641 [30] K. Huber, (1993), Calcium-induced shrinking of polyacrylate chains in aqueous solution, *J. Phys.*  
642 *Chem.*, 97, 38, 9825-9830
- 643 [31] R. Schweins, K. Huber (2001), Collapse of sodium polyacrylate chains in calcium salt solutions, *Eur.*  
644 *Phys. J. E*, 5, 1, 117-126
- 645 [32] X.F. Song, J.F. Wei, T. Sh. He (2009), A method to repair concrete leakage through cracks by  
646 synthesizing super-absorbent resin in situ, *Construction and Building Materials*, 23, 386-391
- 647 [33] H.X.D. Lee (2011), Self-sealing of cracks in cement-based materials using superabsorbent polymers.  
648 PhD thesis. London, Imperial College London.
- 649 [34] C. Schrofl, V. Mechtcherine, M. Gorges (2012), Relation between the molecular structure and the  
650 efficiency of superabsorbent polymers (SAP) as concrete admixture to mitigate autogenous shrinkage,  
651 *Cem. Concr Res.*, 42, 865-873.
- 652 [35] H.X.D. Lee, H.S. Wong, N.R. Buenfeld (2010), Estimating the swelling ratio of superabsorbent  
653 polymers in cement-based materials, International RILEM Conference on Use of Superabsorbent  
654 Polymers and other New Additives in Concrete, RILEM Publications SARL, 163-170.
- 655 [36] W. Khushefati (2004), Healing of cracks in concrete, Department of Civil and Environmental  
656 Engineering, Imperial College, University of London, PhD Thesis
- 657 [37] R. Bowen (1986), *Groundwater*, 2<sup>nd</sup> Edition, Elsevier Applied Science Publishers Ltd. London.
- 658 [38] H.S. Wong, N.R. Buenfeld (2006), Patch microstructure in cement-based materials: Fact or artefact?  
659 *Cem. Concr. Res.*, 36 [5] 990-997.
- 660 [39] K.L. Scrivener, A.K. Crumbie, P. Laugesen (2004), The interfacial transition zone (ITZ) between  
661 cement paste and aggregate in concrete, *Interface Science*, 12, 411-421.

- 662 [40] H.S. Wong, N.R. Buenfeld (2006), Euclidean Distance Mapping for computing microstructural  
663 gradients at interfaces in composite materials, *Cem. Concr. Res.* 36, 1091-1097.
- 664 [41] H.S. Wong, A.M. Pappas, R.W. Zimmerman, N.R. Buenfeld (2011), Effect of entrained air voids on  
665 the microstructure and mass transport properties of concrete, *Cem. Concr. Res.* 41, 1067-1077.
- 666 [42] E.E. Underwood (1970), *Quantitative Stereology*, Addison-Wesley, Reading, Massachusetts.
- 667 [43] J.C. Russ, R.T. Dehoff (2001), *Practical Stereology*, Second Edition, New York, Plenum Press.
- 668 [44] H-W. Reinhardt, M. Joss (2003), Permeability and self-healing of cracked concrete as a function of  
669 temperature and crack width, *Cem. Concr. Res.*, 33, 981-985.
- 670 [45] H.X.D. Lee, H.S. Wong, N.R. Buenfeld (2015), Effect of alkalinity and calcium content on the  
671 swelling of superabsorbent polymers in cement paste, *In preparation*.
- 672 [47] R.D. Toledo Filho, E.F. Silva, A.N.M. Lopes, V. Mechtcherine, and L. Dudziak (2012), Effect of  
673 superabsorbent polymers on the workability of concrete and mortar, In: *Application of superabsorbent*  
674 *polymers (SAP) in concrete construction*, V. Mechtcherine & H.W. Reinhardt (Editors), State-of-the-  
675 art report, Springer.
- 676 [48] J. Justs, M. Wyrzykowski, D. Bajare P. Lura (2015), Internal curing by superabsorbent polymers in  
677 ultra-high performance concrete, *Cem. Concr. Res.*, 76, 82-90.
- 678 [49] K. Kovler (2012), Effect of superabsorbent polymers on the mechanical properties of concrete, In:  
679 *Application of superabsorbent polymers (SAP) in concrete construction*, V. Mechtcherine & H.W.  
680 Reinhardt (Editors), State-of-the-art report, Springer.
- 681 [50] M.T. Hasholt, M.H.S. Jespersen, O.M. Jensen (2010), Mechanical properties of concrete with SAP  
682 Part 1: Development of compressive strength, *International RILEM Conference on Use of*  
683 *Superabsorbent Polymers and other New Additives in Concrete*, RILEM Publications SARL, 117-126.
- 684
- 685

686

687

688

689

690

691

692

693

694

695 **Table 1 Oxide composition of Portland cements used**

Cement	Oxide composition (%)										
	SiO <sub>2</sub>	Al <sub>2</sub> O <sub>3</sub>	Fe <sub>2</sub> O <sub>3</sub>	CaO	MgO	SO <sub>3</sub>	K <sub>2</sub> O	Na <sub>2</sub> O	EqNa <sub>2</sub> O	P <sub>2</sub> O <sub>5</sub>	Free CaO
<b>CEM I (white)</b>	24.0	3.63	0.47	69.6	0.69	2.21	0.12	0.01	0.09	0.56	2.0
<b>CEM II</b>	29.1	10.2	4.1	48.5	1.1	2.9	1.22	0.37	1.17	0.26	-

696

697 **Table 2 Particle size distribution, specific gravity and water absorption of the aggregates (quartz**  
698 **sharp sand and Thames Valley gravel) used**

	Cumulative percentage passing at sieve size (in mm)									Specific gravity		24-hr absorption (%)
	14	10	5	2.36	1.18	0.6	0.3	0.15	0.063	(oven-dry)	(SSD)	
Sand	-	-	99.2	86.2	77.0	66.7	23.8	4.19	1.87	2.73	2.75	0.6
Gravel	100	91.9	9.17	1.26	0.73	0.50	0.23	0.06	-	2.76	2.81	1.6

699

700 **Table 3 Properties of the SAP used**

SAP	Source	Diameter (μm)	Bulk density	Polymer type	Swelling ratio, g/g
-----	--------	---------------	--------------	--------------	---------------------

					(kg/m <sup>3</sup> )			
					Deionised water	0.12 wt% NaCl	Synthetic groundwater	Synthetic pore solution
S1	BASF	<100	600-700	Poly(AA)	214	77	64	16
S2	Evonik	100-300	n/a	Poly(AA)	222	79	89	21
S3	ETi	100-500	420	Poly(AA)	259	82	85	22
S5	ETi	1-200	540	Poly(AA-co-AM)	208	73	71	23

701

702

703

704

705

706

707

708 **Table 4 Cement paste, mortar and concrete mix proportions**

Specimen	ID	Cement type	Free w/c	Total w/c	Swelling ratio, $S_I$	Batch quantities (kg/m <sup>3</sup> )			
						Cement	SAP	Sand	Gravel
<i>Series I:</i>									
1. Cement paste (control)	CP1	CEM II	0.30	0.30	-	1557	-	-	-
2. Cement paste - 5% S1	CP1-5S1	CEM II	0.30	0.65	7	978	48.9	-	-
3. Cement paste - 5% S2	CP1-5S2	CEM II	0.30	0.75	9	891	44.5	-	-
4. Cement paste - 5% S3	CP1-5S3	CEM II	0.30	0.75	9	891	44.5	-	-
5. Cement paste - 4% S5	CP1-4S5	CEM II	0.30	1.10	20	682	27.3	-	-
<i>Series II:</i>									
6. Cement paste (control)	CP2	CEM I	0.30	0.30	-	1590	-	-	-
7. Cement paste (control)*	CP2*	CEM I	0.30	0.30	-	1526	-	-	-
8. Cement paste - 13% S2*	CP2-13S2*	CEM I	0.30	0.75	3.5	826	112	-	-
9. Cement paste - 8% S5*	CP2-8S5*	CEM I	0.30	0.75	5.6	853	71.1	-	-
<i>Series III:</i>									
10. Mortar (control)	M	CEM II	0.50	0.50	-	593	-	1365	-
11. Mortar - 5% S1	M-5S1	CEM II	0.50	0.85	7	409	20.5	1365	-
12. Mortar - 5% S2	M-5S2	CEM II	0.50	1.10	12	340	17.0	1365	-

*Series IV:*

13. Concrete (control) *	C*	CEM I	0.40	0.40	-	461	-	630	1160
14. Concrete - 13% S2*	C-13S2*	CEM I	0.40	1.11	5.3	225	30.4	630	1160
15. Concrete - 8% S5*	C-8S5*	CEM I	0.40	1.12	8.6	224	18.7	630	1160

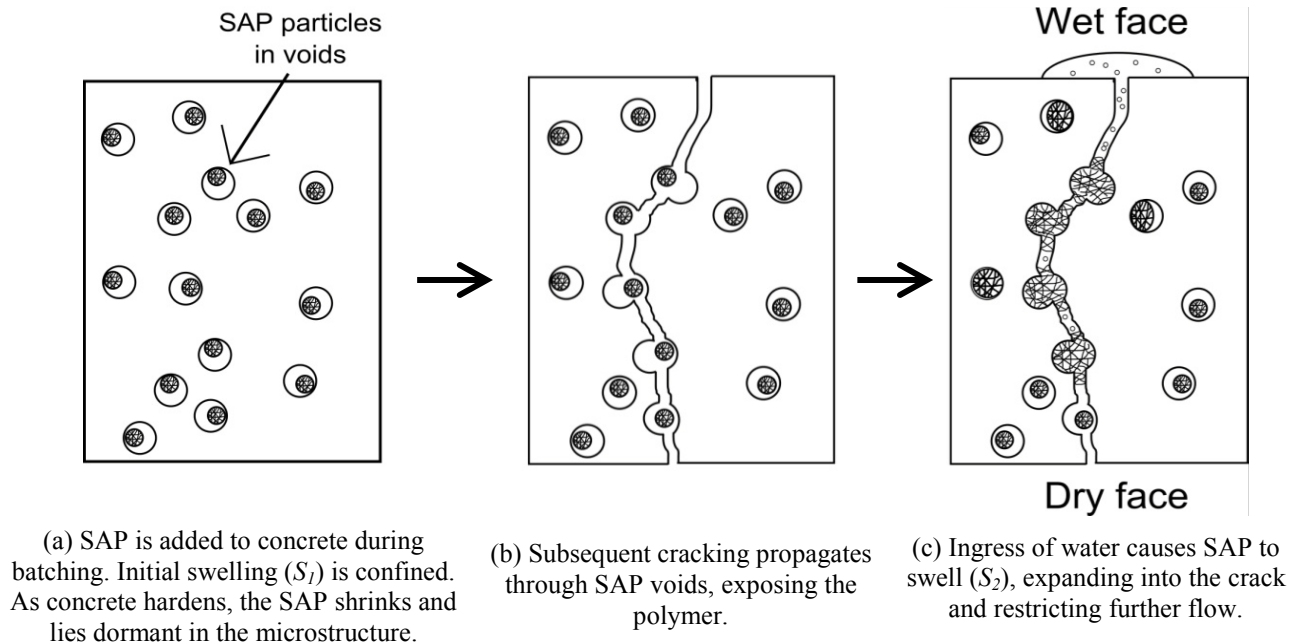
709 Notes: \* Mixes marked with asterisk contain 4% calcium nitrate by weight of cement.

710

711 **Table 5 Effect of high SAP dosages on 28-day compressive strength**

Specimen	ID	w/c	Average strength (N/mm <sup>2</sup> )	Total strength decrease (%)	Strength decrease per 1% SAP (%)
Cement paste (control)	CP1	0.3	77.6 (1.7)	-	-
Cement paste – 5% S2	CP1-5S2	0.3	10.0 (0.3)	87.1	17.4
Cement paste (control)*	CP2*	0.3	86.9 (1.3)	-	-
Cement paste – 13% S2*	CP2-13S2*	0.3	10.9 (0.1)	87.4	6.7
Mortar (control)	M	0.5	40.3 (1.8)	-	-
Mortar - 5% S2	M-5S2	0.5	8.1 (0.2)	79.9	16.0
Concrete (control)*	C*	0.4	74.7 (1.2)	-	-
Concrete – 13% S2*	C-13S2*	0.4	10.6 (0.3)	85.8	6.6

712 Notes: Standard deviation shown in parentheses. Mixes marked with asterisk contain 4% calcium nitrate by  
713 weight of cement

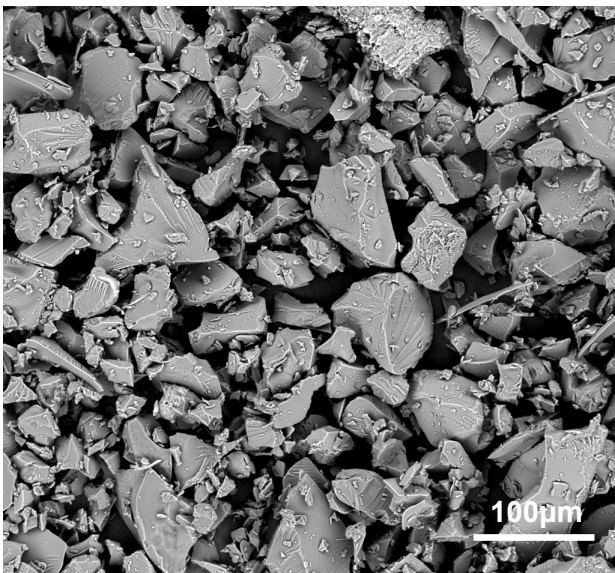


714 **Fig. 1 Schematic of the crack self-sealing mechanism using SAP [23].**

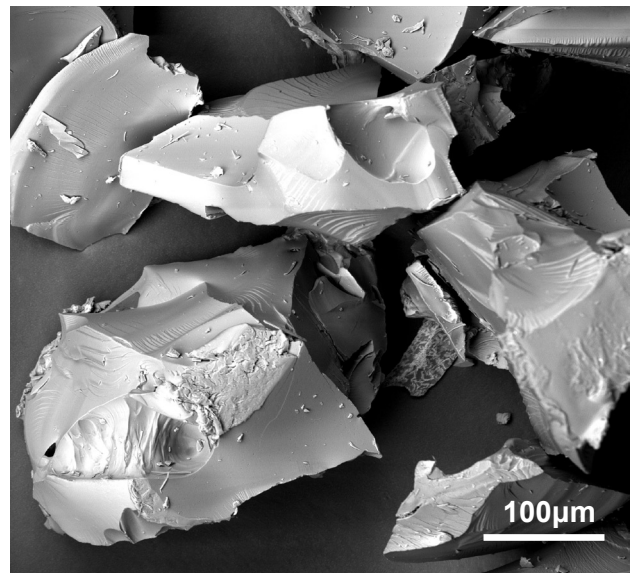
715

716

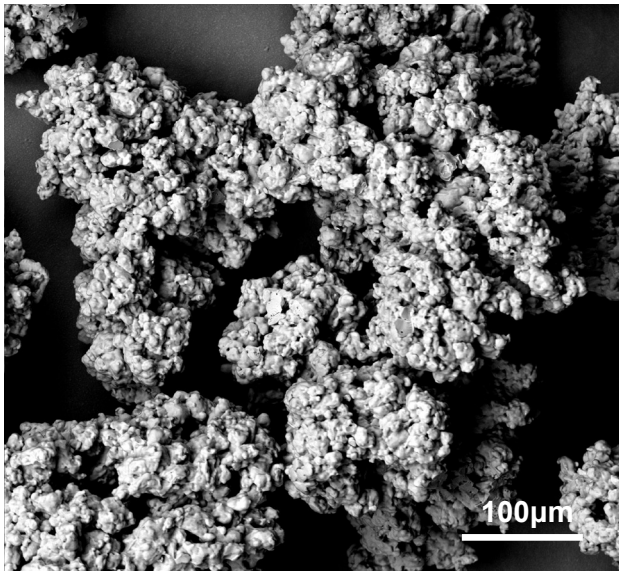
717  
718  
719  
720  
721  
722  
723  
724  
725  
726  
727  
728  
729  
730  
731  
732  
733  
734  
735  
736



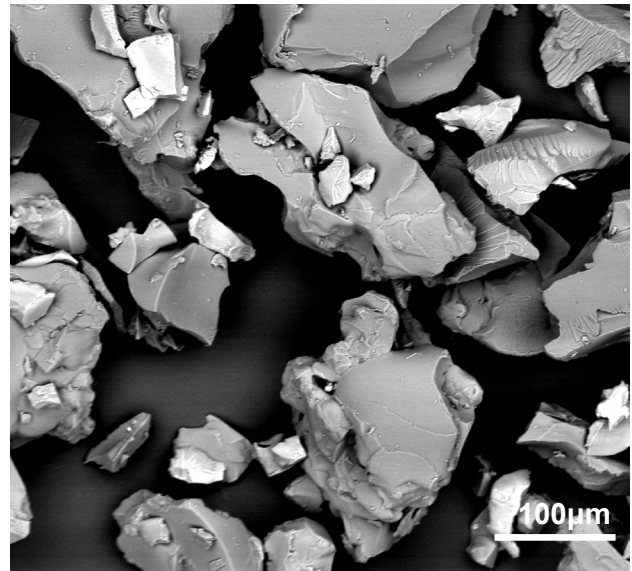
(a) S1



(b) S2



(c) S3

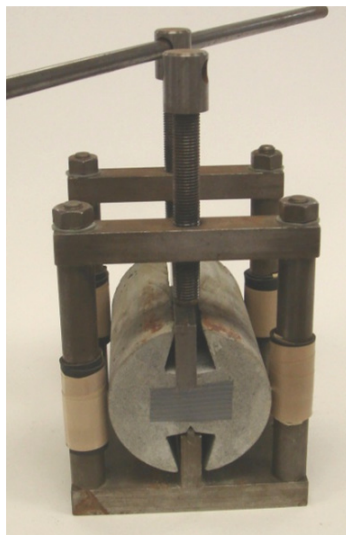


(d) S5

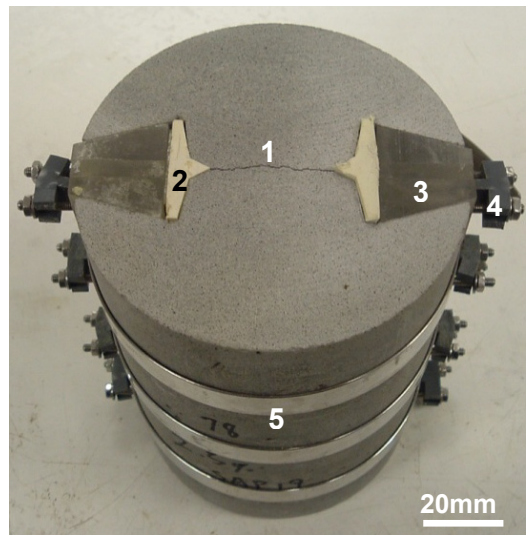
737 **Fig 2** Scanning electron micrographs show that S1, S2 and S5 consist of smooth angular particles while  
738 S3 particles are rough textured with an agglomerate structure. S1 has the smallest particle size.  
739



(a)



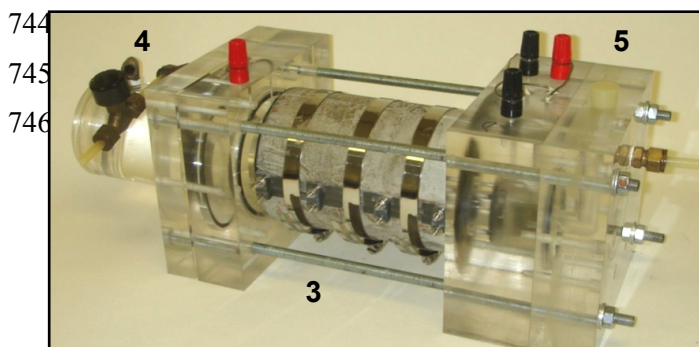
(b)



(c)

740 **Fig. 3** a) Casting mould with trapezoid inserts, b) loading device to induce a single through crack, and  
741 c) top view of the assembled cracked sample showing induced crack (1), silicone rubber seal (2),  
742 Perspex trapezoidal insert (3), tightening nut (4) and hose clamp (5).

743





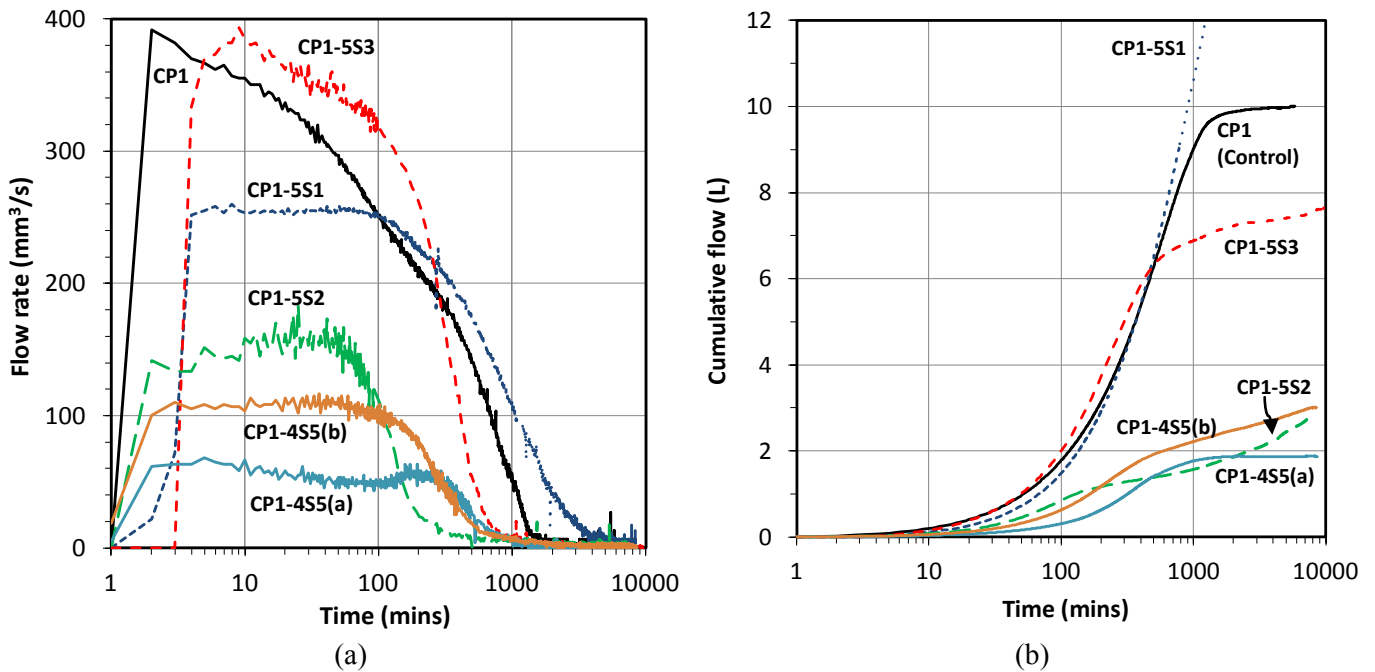
747

748

749

750

**Fig. 4** Setup for the flow through crack (FTC) experiment which consists of the upper tank filled with 0.02M NaCl solution (1), pump (2), assembled specimen (3), inlet (4) and outlet (5) cells, lower tank (6) and electronic balance (7) connected to data loggers (not shown).

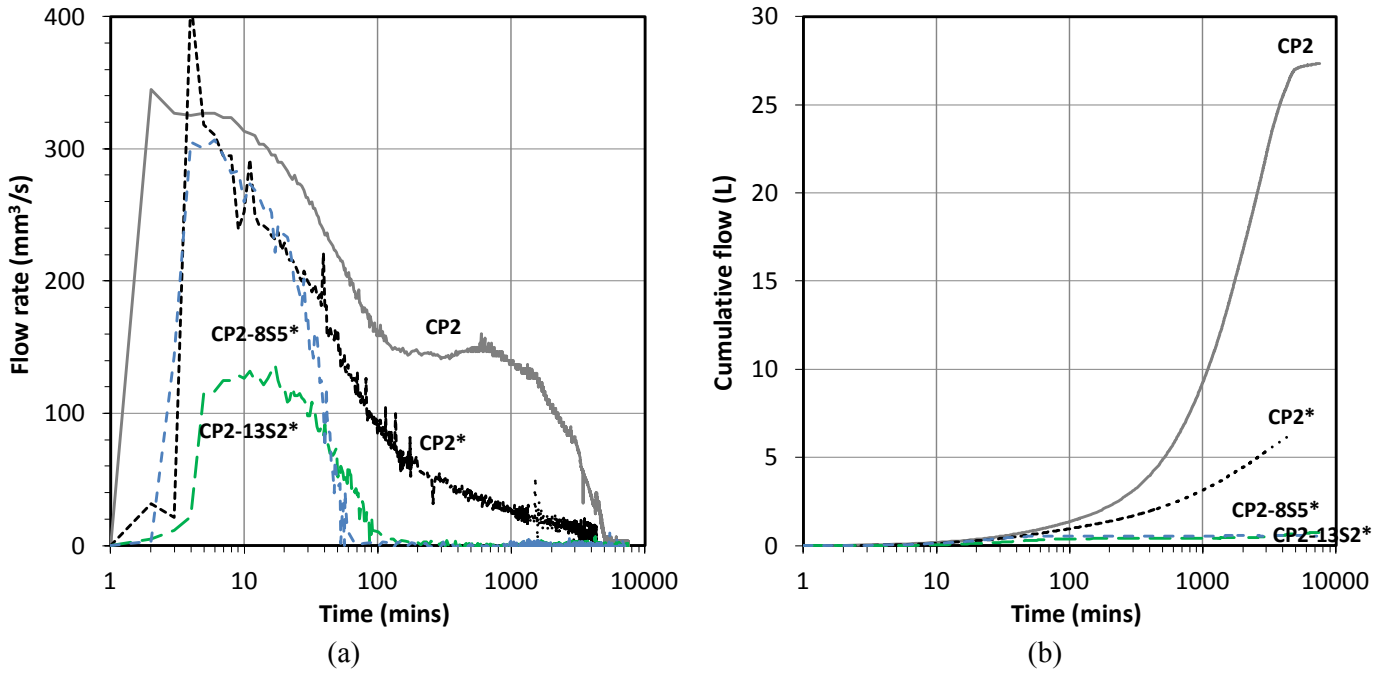


751

752

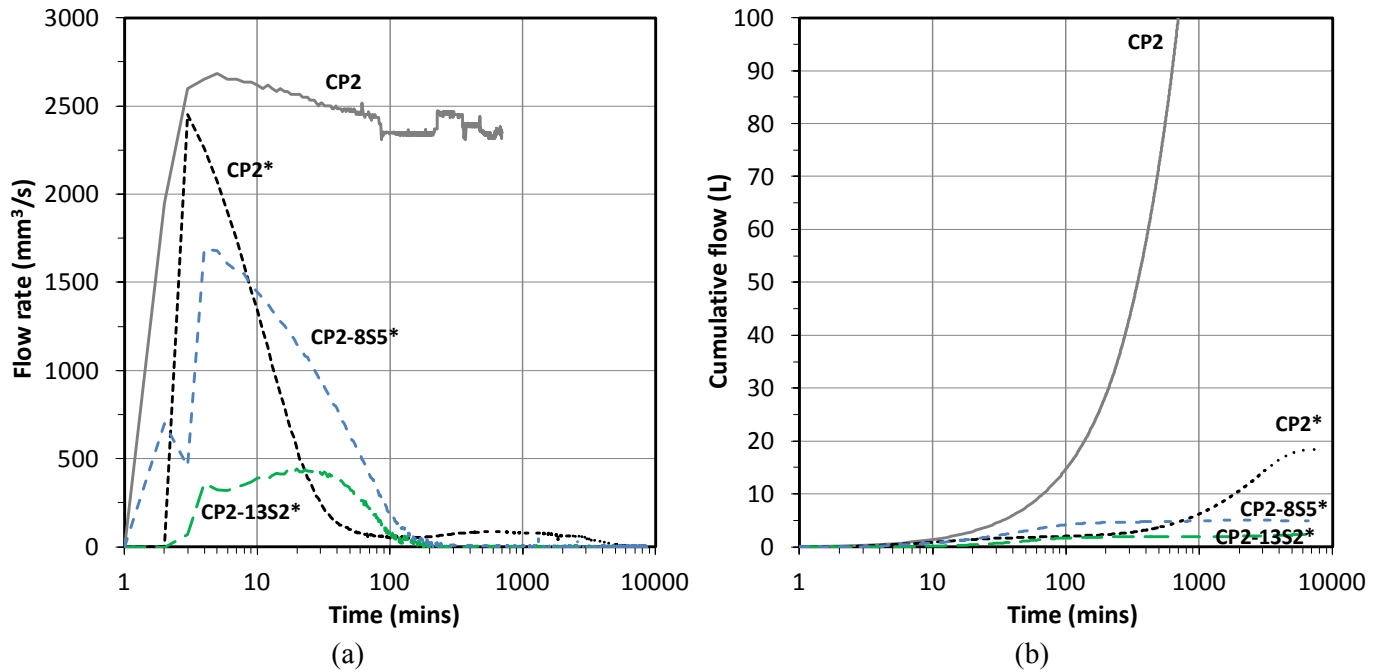
753

**Fig. 5** Flow rate (a) and cumulative flow (b) of NaCl through a 0.2 mm crack for pastes from Series I (w/c 0.3).



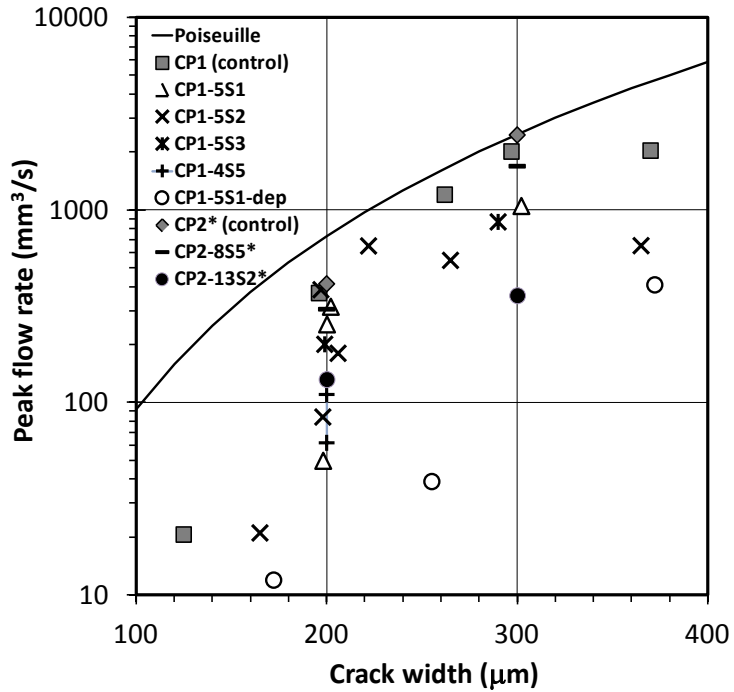
754 **Fig. 6** Flow rate (a) and cumulative flow (b) of NaCl through a 0.2 mm crack for pastes from Series II  
 755 (w/c 0.3). Mixes marked with asterisk contain 4% calcium nitrate.

756



757 **Fig. 7** Flow rate (a) and cumulative flow (b) of NaCl through a 0.3 mm crack for pastes from Series II  
 758 (w/c 0.3).

759

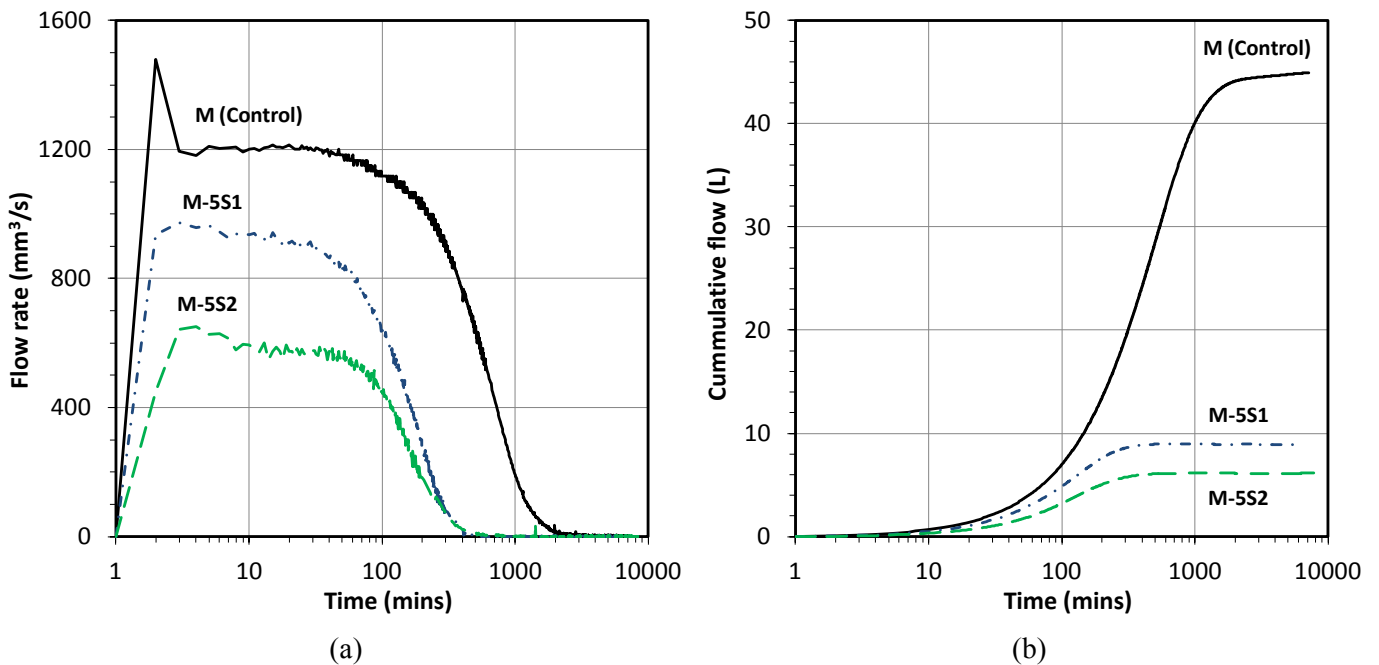


760

761

**Fig. 8 Influence of crack width on the peak flow rate for pastes from Series I & II (w/c 0.3).**

762



763

764

**Fig. 9 Flow rate (a) and cumulative flow (b) of NaCl through a 0.3 mm crack for mortars from Series III (w/c 0.5).**

765

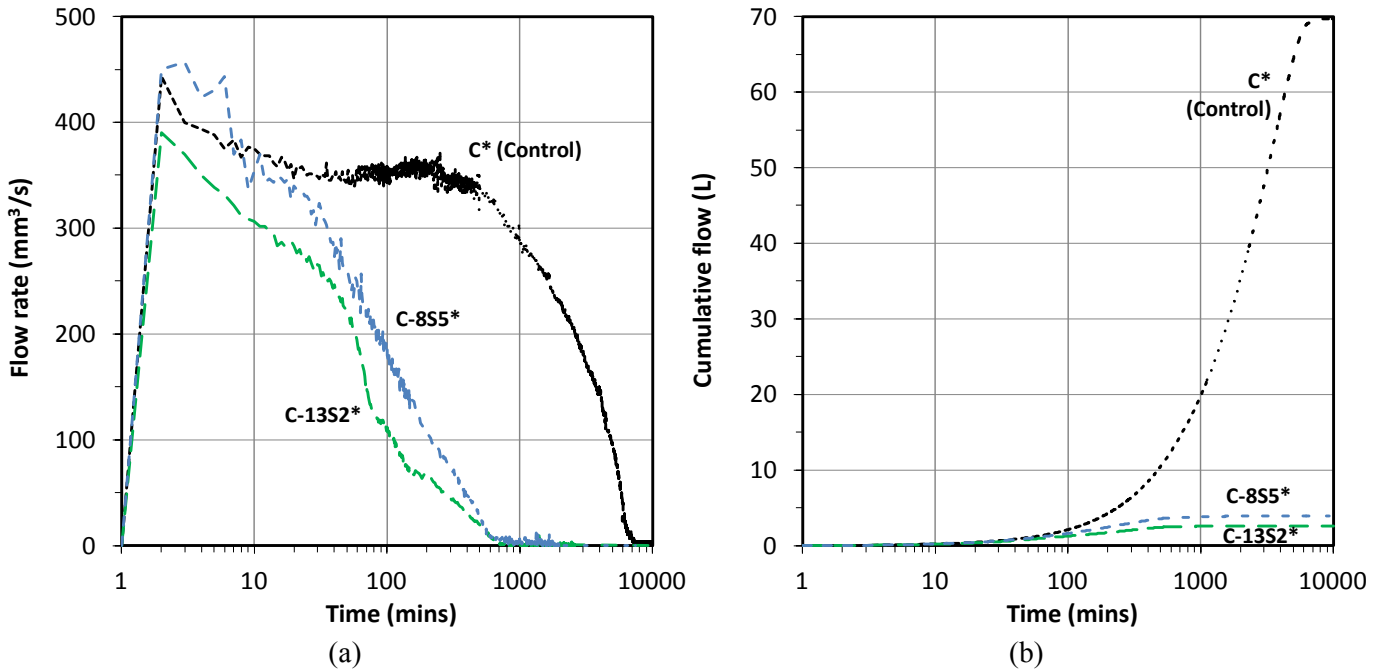


Fig. 10 Flow rate (a) and cumulative flow (b) of NaCl through a 0.3 mm crack for concretes from Series IV (w/c 0.4).

766  
767  
768

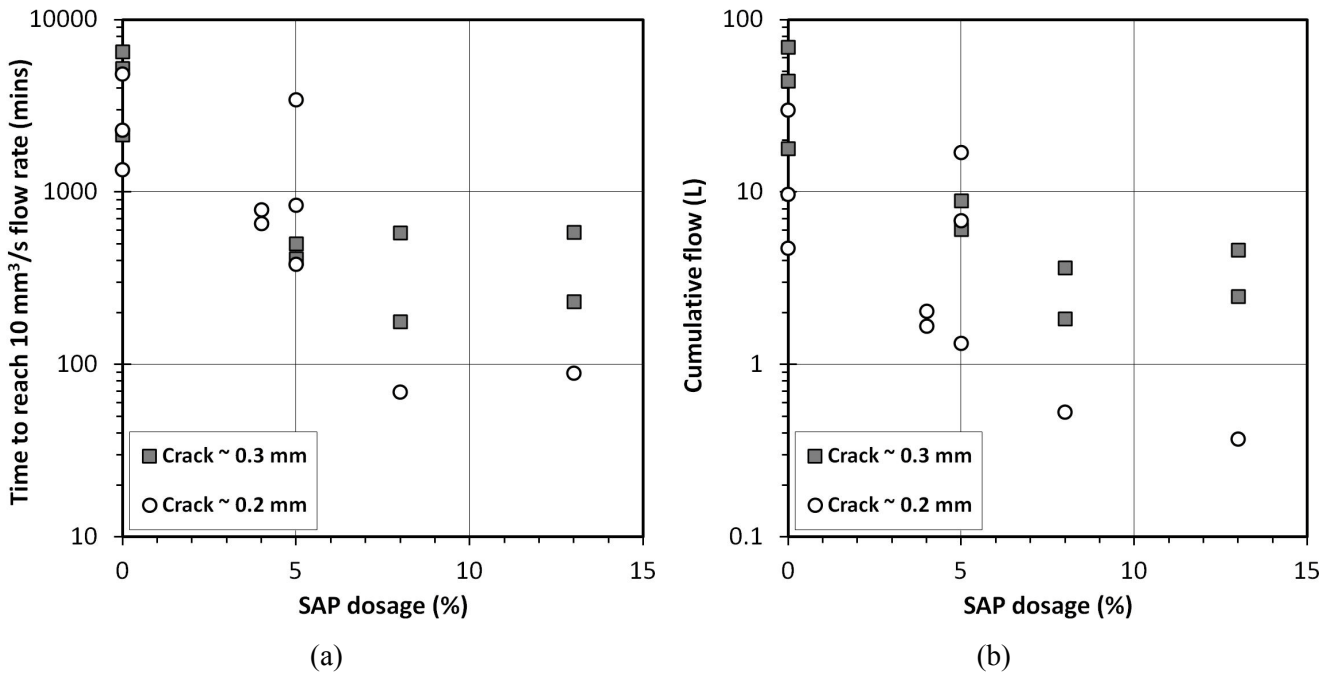


Fig. 11 Effect of SAP dosage (% wt. of cement) on a) the time to reach negligible flow rate (= 10 mm<sup>3</sup>/s) and b) cumulative flow for all specimens.

769  
770  
771  
772

773

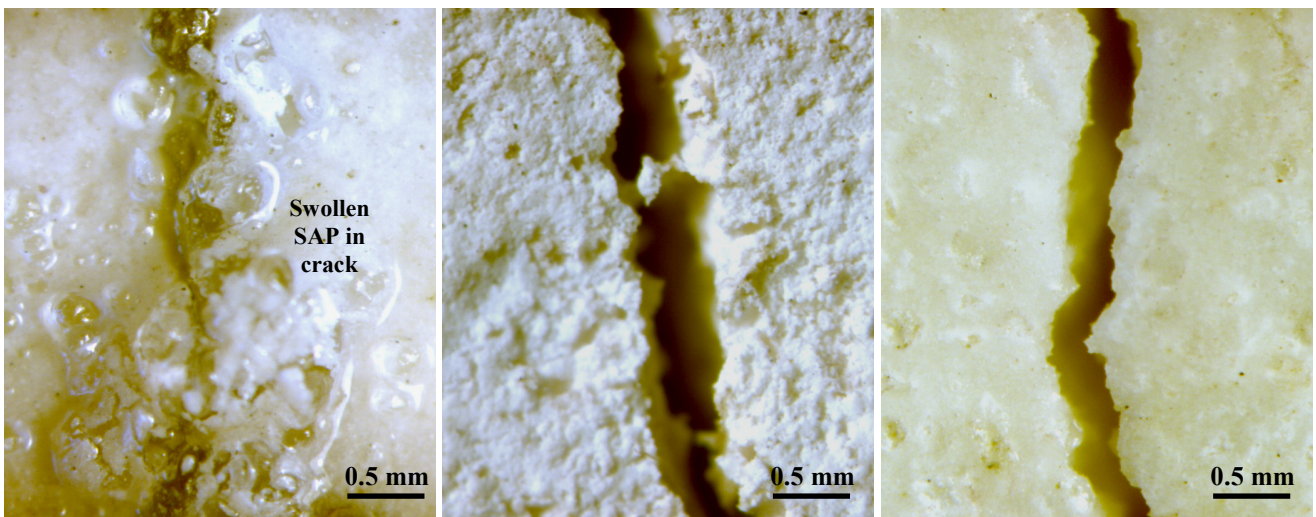
774

775

776

777

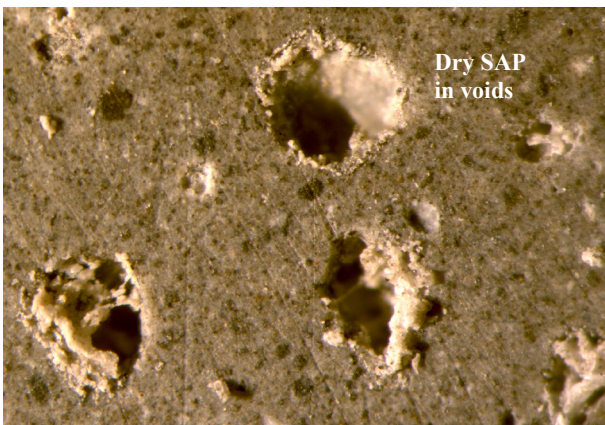
778



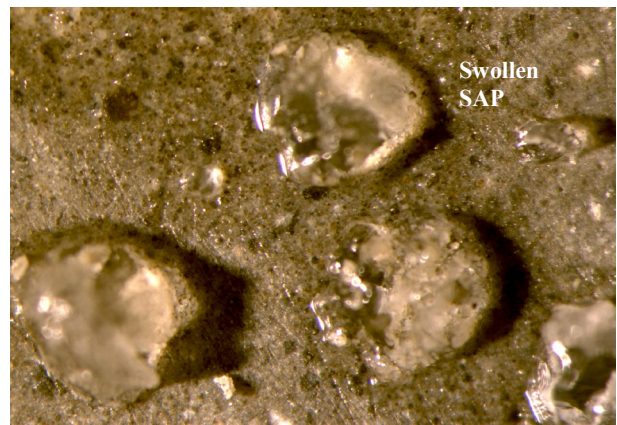
a) Upstream face, imaged immediately after FTC experiment showing the swollen SAP in crack.

b) Upstream face, imaged after FTC experiment and drying at room temperature for 24 hours

c) Downstream face, imaged immediately after FTC experiment



d) Before wetting



e) After wetting

779

780

**Fig. 12 Stereo micrographs of a sealed crack after the FTC experiment, specimen is CP2-8S5\*. Figures (d) and (e) show close-up area matching stereo micrographs of crack surface before and after wetting.**

781

782

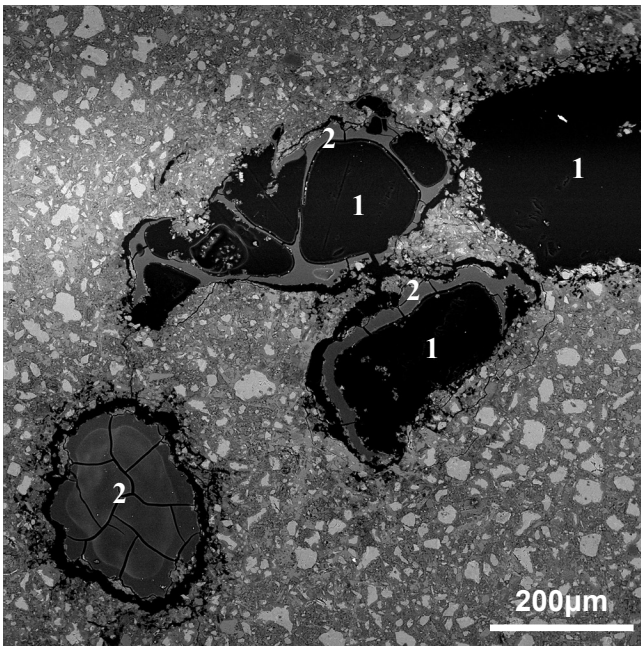
783

784

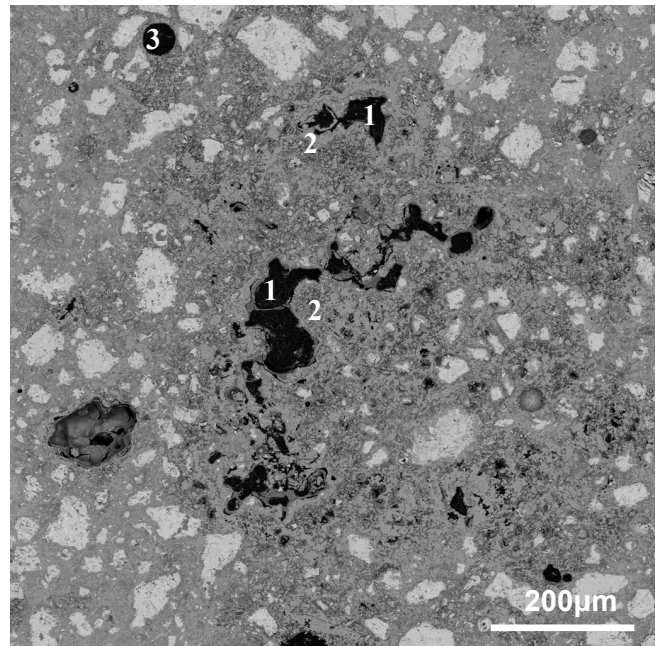
785

786

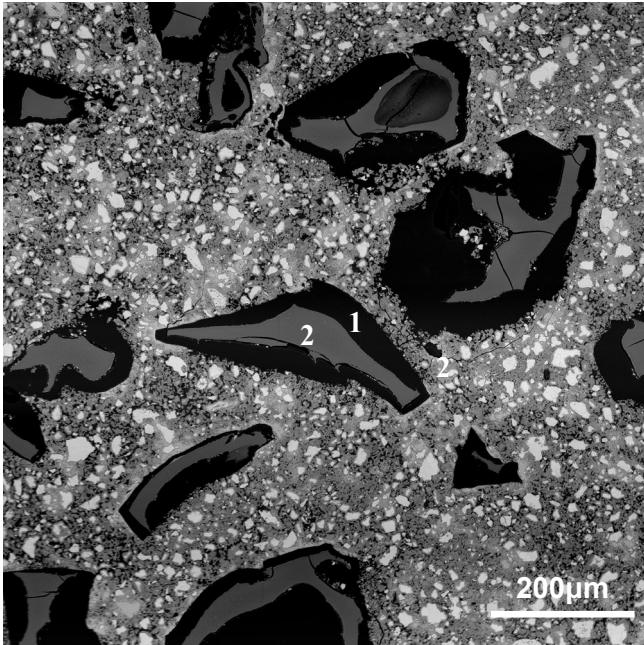
787



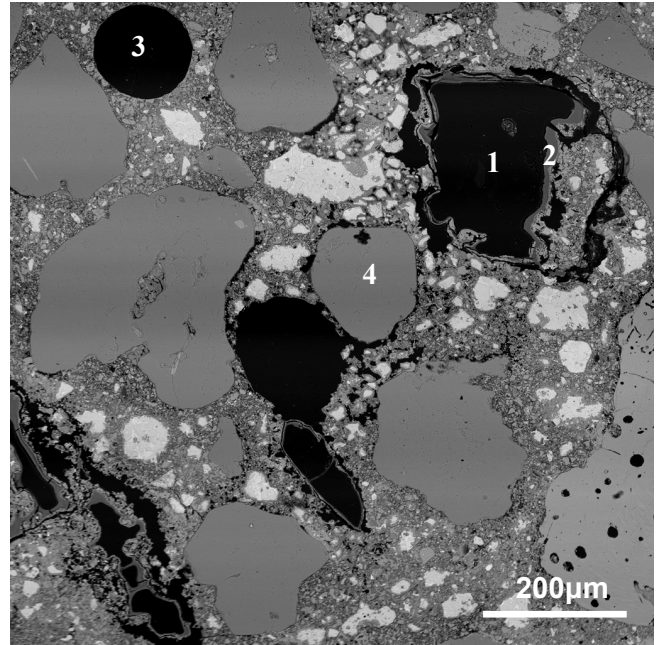
(a) CP1-5S2



(b) CP1-5S3



(c) CP2-13S2\*



(d) M-5S2

788

789

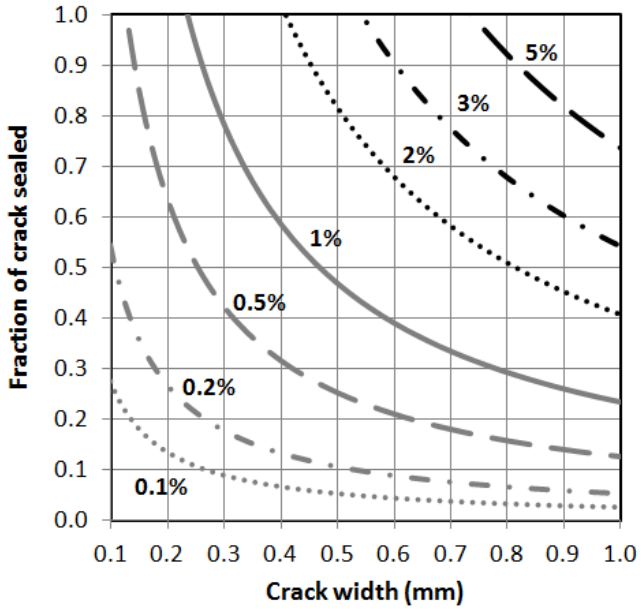
790

791

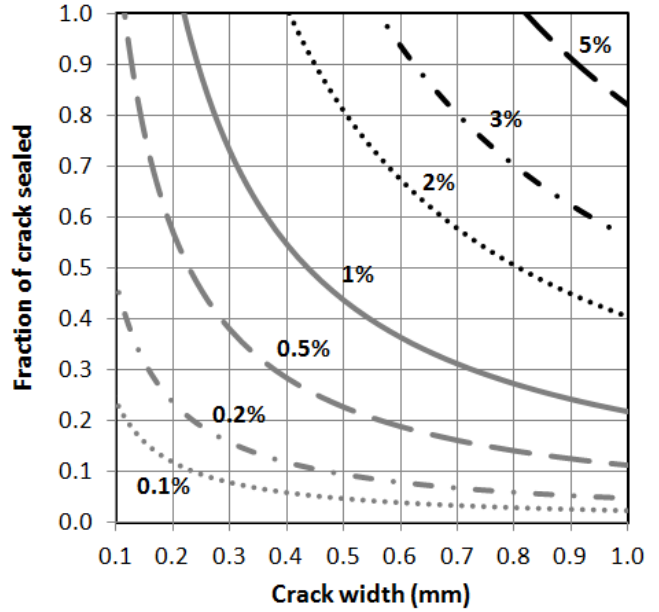
792

793

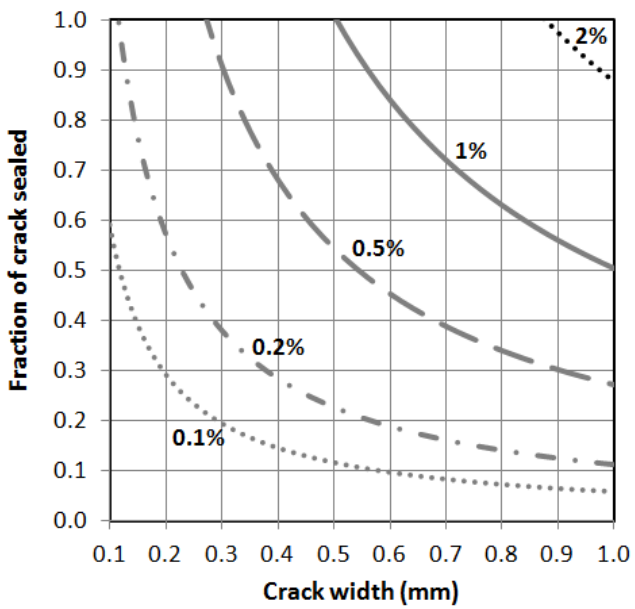
**Fig. 13 Selection of images from BSE microscopy showing the effect of SAP on microstructure of cement-based materials. The micrographs highlight the SAP voids (1), remnants of the collapsed SAP (2), entrapped air (3), aggregate particles (4) and the SAP/cement paste interface.**



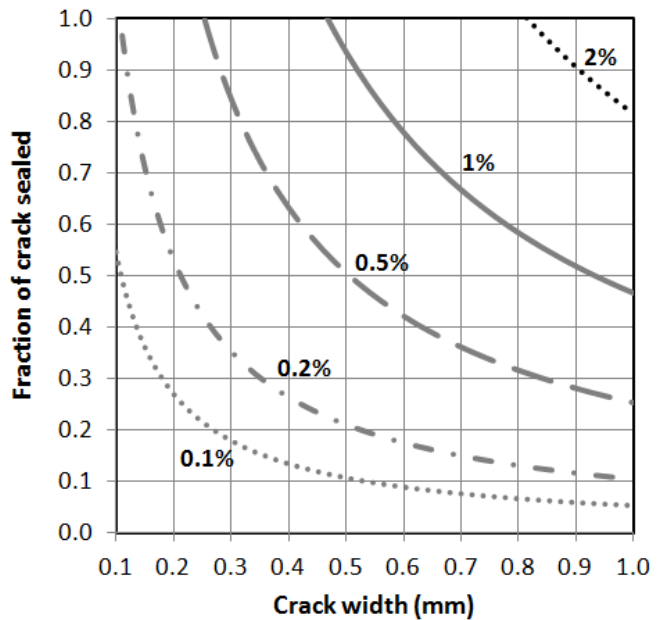
(a)  $S_1 = 10 \text{ g/g}$ ,  $S_2 = 75 \text{ g/g}$ ,  $d_o = 100 \mu\text{m}$



(b)  $S_1 = 5 \text{ g/g}$ ,  $S_2 = 75 \text{ g/g}$ ,  $d_o = 100 \mu\text{m}$



(c)  $S_1 = 10 \text{ g/g}$ ,  $S_2 = 150 \text{ g/g}$ ,  $d_o = 100 \mu\text{m}$



(d)  $S_1 = 10 \text{ g/g}$ ,  $S_2 = 75 \text{ g/g}$ ,  $d_o = 200 \mu\text{m}$

794 **Fig. 14 Modelling of the crack fraction sealed as a function of crack width and SAP dosage ( $\alpha$ , wt% of**  
 795 **cement) for a cement paste at 0.3 w/c ratio. Results show that crack sealing can be enhanced by**  
 796 **depressing the initial swelling ratio  $S_1$  (Fig. b), increasing the subsequent swelling ratio  $S_2$  in crack (Fig.**  
 797 **c) and increasing the particle size of SAP,  $d_o$  (Fig. d).**

798

799

800

